

ISO-SWS calibration and the accurate modelling of cool-star atmospheres ^{*}

III. A0 – G2 stars: APPENDIX

L. Decin^{1**}, B. Vandenbussche¹, C. Waelkens¹, K. Eriksson², B. Gustafsson², B. Plez³, and A.J. Sauval⁴

¹ Instituut voor Sterrenkunde, KULeuven, Celestijnenlaan 200B, B-3001 Leuven, Belgium

² Institute for Astronomy and Space Physics, Box 515, S-75120 Uppsala, Sweden

³ GRAAL - CC72, Université de Montpellier II, F-34095 Montpellier Cedex 5, France

⁴ Observatoire Royal de Belgique, Avenue Circulaire 3, B-1180 Bruxelles, Belgium

Received data; accepted date

Abstract. Vega, Sirius, β Leo, α Car and α Cen A belong to a sample of twenty stellar sources used for the calibration of the detectors of the Short-Wavelength Spectrometer on board the Infrared Space Observatory (ISO-SWS). While general problems with the calibration and with the theoretical modelling of these stars are reported in Decin et al. (2002), each of these stars is discussed individually in this paper. As demonstrated in Decin et al. (2002), it is not possible to deduce the effective temperature, the gravity and the chemical composition from the ISO-SWS spectra of these stars. But since ISO-SWS is absolutely calibrated, the angular diameter (θ_d) of these stellar sources can be deduced from their ISO-SWS spectra, which consequently yields the stellar radius (R), the gravity-inferred mass (M_g) and the luminosity (L) for these stars. For Vega, we obtained $\theta_d = 3.35 \pm 0.20$ mas, $R = 2.79 \pm 0.17 R_\odot$, $M_g = 2.54 \pm 1.21 M_\odot$ and $L = 61 \pm 9 L_\odot$; for Sirius $\theta_d = 6.17 \pm 0.38$ mas, $R = 1.75 \pm 0.11 R_\odot$, $M_g = 2.22 \pm 1.06 M_\odot$ and $L = 29 \pm 6 L_\odot$; for β Leo $\theta_d = 1.47 \pm 0.09$ mas, $R = 1.75 \pm 0.11 R_\odot$, $M_g = 1.78 \pm 0.46 M_\odot$ and $L = 15 \pm 2 L_\odot$; for α Car $\theta_d = 7.22 \pm 0.42$ mas, $R = 74.39 \pm 5.76 R_\odot$, $M_g = 12.80^{+24.95}_{-6.35} M_\odot$ and $L = 14573 \pm 2268 L_\odot$ and for α Cen A $\theta_d = 8.80 \pm 0.51$ mas, $R = 1.27 \pm 0.08 R_\odot$, $M_g = 1.35 \pm 0.22 M_\odot$ and $L = 1.7 \pm 0.2 L_\odot$. These deduced parameters are confronted with other published values and the goodness-of-fit between observed ISO-SWS data and the corresponding synthetic spectrum is discussed.

Key words. Infrared: stars – Stars: atmospheres – Stars: fundamental parameters – Stars: individual: Vega, Sirius, Denebola, Canopus, α Cen A

Appendix A: Comparison between different ISO-SWS and synthetic spectra (coloured plots)

In this section, Fig. ?? – Fig. ??, Fig. ?? – Fig. ?? of the accompanying article are plotted in colour in order to better distinguish the different observational or synthetic spectra.

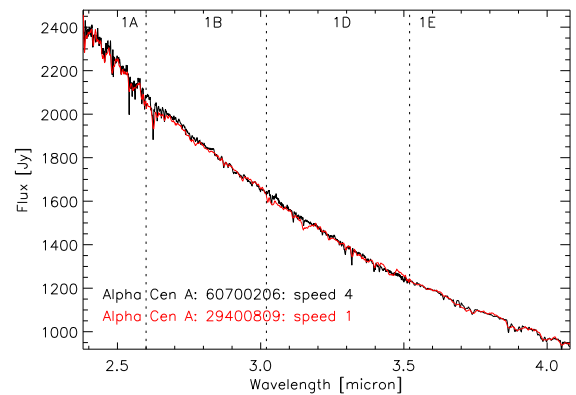


Fig. A.1. Comparison between the AOT01 speed-4 observation of α Cen A (revolution 607) and the speed-1 observation (revolution 294). The data of the speed-1 observation have been multiplied by a factor 1.16.

Send offprint requests to: L. Decin, e-mail: Leen.Decin@ster.kuleuven.ac.be

^{*} Based on observations with ISO, an ESA project with instruments funded by ESA Member States (especially the PI countries France, Germany, the Netherlands and the United Kingdom) and with the participation of ISAS and NASA.

^{**} Postdoctoral Fellow of the Fund for Scientific Research, Flanders

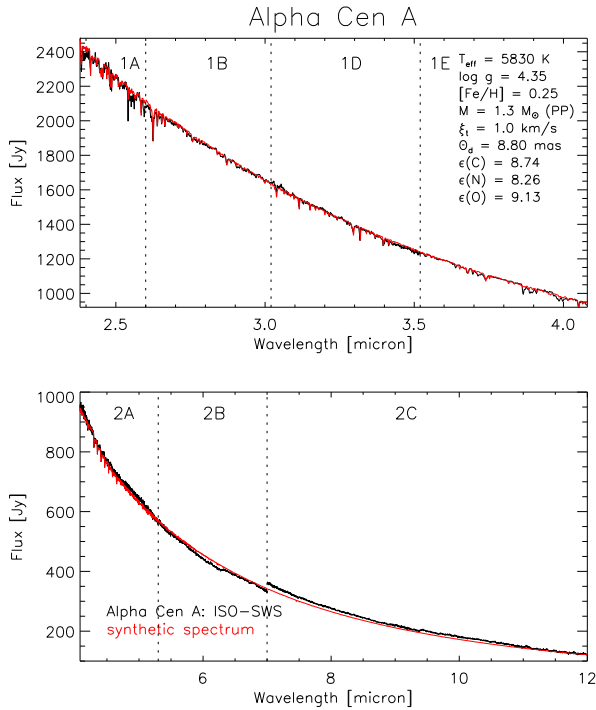


Fig. A.2. Comparison between band 1 and band 2 of the ISO-SWS data of α Cen A (black) and the synthetic spectrum (red) with stellar parameters $T_{\text{eff}} = 5830$ K, $\log g = 4.35$, $M = 1.3 M_{\odot}$, $[\text{Fe}/\text{H}] = 0.25$, $\xi_t = 1.0 \text{ km s}^{-1}$, $\epsilon(\text{C}) = 8.74$, $\epsilon(\text{N}) = 8.26$, $\epsilon(\text{O}) = 9.13$ and $\theta_d = 8.80$ mas.

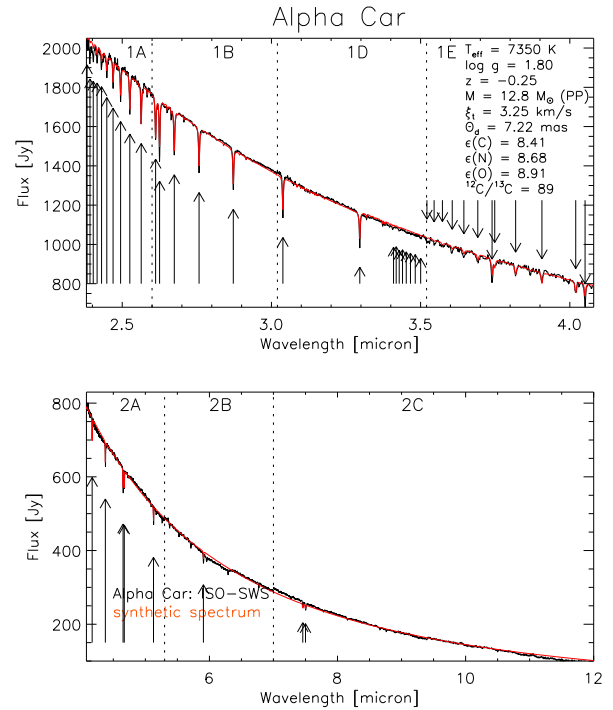


Fig. A.3. Comparison between band 1 and band 2 of the ISO-SWS data of α Car (black) and the synthetic spectrum (red) with stellar parameters $T_{\text{eff}} = 7350$ K, $\log g = 1.80$, $M = 12.8 M_{\odot}$, $[\text{Fe}/\text{H}] = -0.25$, $\xi_t = 3.25 \text{ km s}^{-1}$, $\epsilon(\text{C}) = 8.41$, $\epsilon(\text{N}) = 8.68$, $\epsilon(\text{O}) = 8.91$ and $\theta_d = 7.22$ mas. Hydrogen lines are indicated by arrows.

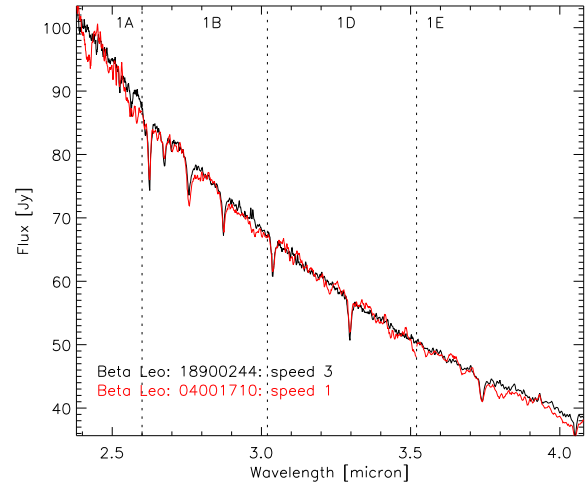


Fig. A.4. Comparison between the AOT01 speed-3 observation of β Leo (revolution 189) and the speed-1 observation (revolution 040). The data of the speed-1 observation have been multiplied by a factor 1.05.

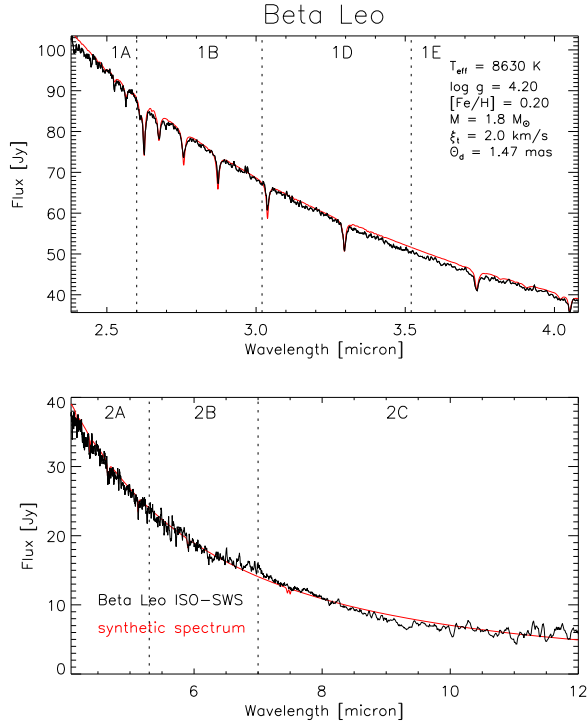


Fig. A.5. Comparison between band 1 and band 2 of the ISO-SWS data of β Leo (black) and the synthetic spectrum (red) with stellar parameters $T_{\text{eff}} = 8630\text{K}$, $\log g = 4.20$, $M = 1.8 M_{\odot}$, $[\text{Fe}/\text{H}] = 0.20$, $\xi_t = 2.0\text{ km s}^{-1}$ and $\theta_d = 1.47\text{ mas}$.

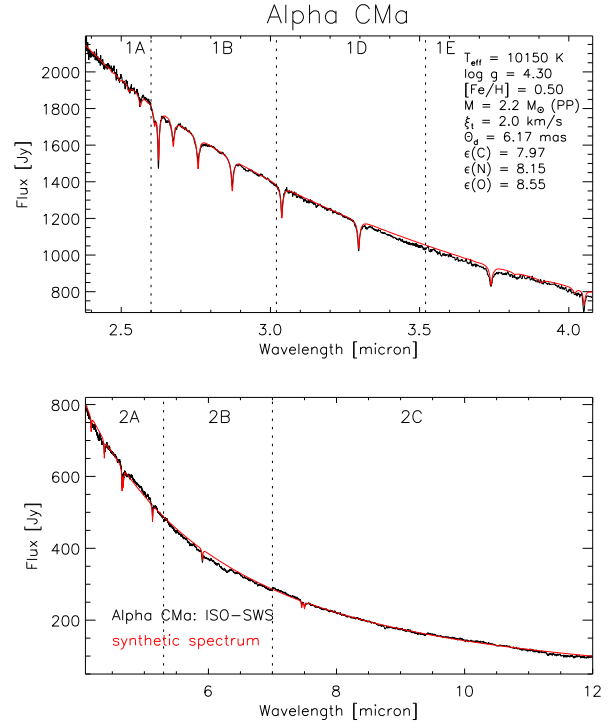


Fig. A.7. Comparison between band 1 and band 2 of the ISO-SWS data of α CMa (black) and the synthetic spectrum (red) with stellar parameters $T_{\text{eff}} = 10150\text{K}$, $\log g = 4.30$, $M = 2.2 M_{\odot}$, $[\text{Fe}/\text{H}] = 0.50$, $\xi_t = 2.0\text{ km s}^{-1}$, $\varepsilon(\text{C}) = 7.97$, $\varepsilon(\text{N}) = 8.15$, $\varepsilon(\text{O}) = 8.55$ and $\theta_d = 6.17\text{ mas}$.

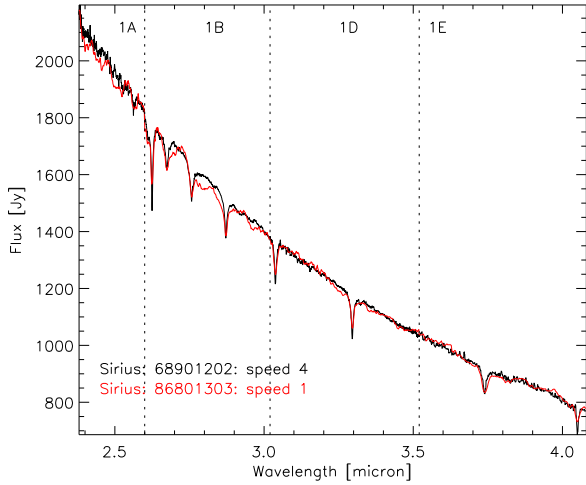


Fig. A.6. Comparison between the AOT01 speed-4 observation of α CMa (revolution 689) and the speed-1 observation (revolution 868). The data of the speed-1 observation have been multiplied by a factor 1.12.

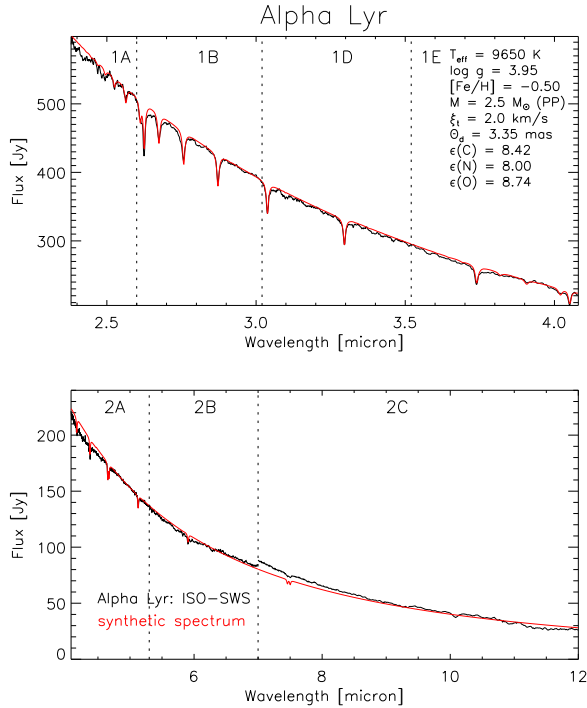
Appendix B: Comments on published stellar parameters

In this appendix, a description of the results obtained by different authors using various methods is given in chronological order. One either can look to the quoted reference in the accompanying paper and then search the description in the chronological (and then alphabetical) listing below or one can use the cross-reference table (Table B.1) to find all the references for one specific star in this numbered listing.

1. Brown et al. (1974) have used the stellar interferometer at Narrabri Observatory to measure the apparent angular diameter of 32 stars. The limb-darkening corrections were based on model atmospheres.
2. Code et al. (1976) have derived the effective temperature from the absolute flux distribution and the apparent angular diameter (Brown et al. 1974). The absolute flux distribution has been found by combining observations of ultraviolet flux with ground-based photometry.
3. Blackwell & Shallis (1977) have described the Infrared Flux Method (IRFM) to determine the stellar angular diameters and effective temperatures from absolute infrared photometry. For 28 stars (including α Car, α Boo, α CMa, α Lyr, β Peg, α Cen A, α Tau and γ Dra) the angular diameters are deduced. Only for the first

Table B.1. Cross-reference table in which one can find all the numbers referring to the papers citing a particular star.

name	reference number
α Cen A	3, 4, 5, 10, 21, 24, 25, 27, 28, 33, 35, 38, 41, 42, 43, 46, 51, 58, 62
α Car	1, 2, 3, 6, 7, 8, 14, 16, 17, 18, 26, 30, 32, 33, 38, 40, 50, 51, 52, 54
β Leo	1, 2, 19, 20, 23, 37, 45, 47, 53, 54, 55, 57, 61
α CMa	1. 8, 2. 11, 3. 12, 4. 15, 5. 19, 6. 20, 7. 31, 8. 33, 9. 36, 10. 44, 11. 54, 12. 56, 13. 59, 14. 60, 15. 64
α Lyr	8, 9, 13, 15, 19, 20, 22, 33, 34, 36, 39, 44, 45, 48, 49, 54, 55, 60, 63, 64

**Fig. A.8.** Comparison between band 1 and band 2 of the ISO-SWS data of α Lyr (black) and the synthetic spectrum (red) with stellar parameters $T_{\text{eff}} = 9650$ K, $\log g = 3.95$, $M = 2.5 M_{\odot}$, $[\text{Fe}/\text{H}] = -0.50$, $\xi_t = 2.0 \text{ km s}^{-1}$, $\epsilon(\text{C}) = 8.42$, $\epsilon(\text{N}) = 8.00$, $\epsilon(\text{O}) = 8.74$ and $\theta_d = 3.35 \text{ mas}$.

four stars the corresponding effective temperatures are computed.

- Using the well-known astrometric properties (e.g. parallax, visual orbit) of the binary α Cen, Flannery & Ayres (1978) have deduced the mass of the A and B component of the binary system. The total and individual masses should be accurate to about 3%, corresponding to the possible 1% error in parallax, while the uncertainty of the mass ratio is somewhat smaller, about 2%. The effective temperature is computed from $(B - V)$ and $(V - I)$ colour indices. For the luminosity different broad-band systems (including the standard *UBV*, the long-wave *RIJKLMN* and the six-colour *UViBGRI*) and narrow-band photometric indices were used. By analysing the temperature sensitive Ca I transition, composition dependent stellar evolution mod-

els and T_{eff} -colour relationships, both the temperature and the (enhanced) metallicity are ascertained.

- Kamper & Wesselink (1978) have determined the proper motion and parallax of the α Centauri system by using all available observations till 1971. The new mass ratio together with the period and the semi-major axis yielded then the total mass of the system and so the individual masses of α Cen A and α Cen B.
- Linsky & Ayres (1978) have estimated the effective temperatures for the programme stars using the mean of the Johnson (1966) $T_{\text{eff}}-(V - I)$ transformations, since these are essentially independent of luminosity.
- Luck (1979) has performed a chemical analysis of nine southern supergiant stars. He obtained spectrograms with the 1.5 m reflector of Cerro Tololo Inter-American observatory. Effective temperature, gravity and micro-turbulent velocity for the programme stars are determined solely in a spectroscopic way from the Fe I and Fe II lines. The equivalent widths are calculated through a model atmosphere with these stellar parameters and are then compared with the observed equivalent widths. The calculation is repeated, changing the abundance of the species under question, until a match is achieved.
- Blackwell et al. (1980) have determined the effective temperature and the angular diameter for 28 stars using the IRFM method.
- Several flux-constant, line-blanketed model stellar atmospheres have been computed for Vega by Dreiling & Bell (1980). The stellar effective temperature has been found by comparisons of observed and computed absolute fluxes. The Balmer line profiles gave the surface gravities, which were consistent with the results from the Balmer jump and with the values found from the radius — deduced from the parallax and the limb-darkened angular diameter — and the (estimated) mass.
- The chemical composition of the major components of the bright, nearby system of α Centauri is derived by England (1980) using high-dispersion spectra. The abundances of 16 elements are found using a differential curve of growth analysis. Scaled solar LTE model atmospheres for α Cen A and α Cen B are calculated using effective temperatures from $H\alpha$ profiles and surface gravities from line profiles and ionisation equilibria.

11. In his review, Popper (1980) has discussed the problems of determining masses from data for eclipsing and visual binaries. Only individual masses of considerable accuracy, determined directly from the observational data, are treated.
12. Several flux-constant, line-blanketed model stellar atmospheres have been computed for Sirius by Bell & Dreiling (1981). The stellar effective temperature has been found by comparisons of observed and computed absolute fluxes. The Balmer line profiles gave the surface gravities, which were consistent with the results from the Balmer jump and with the values found from the radius — deduced from the parallax and the limb-darkened angular diameter — and the (estimated) mass.
13. Sadakane & Nishimura (1981) derived abundances for various elements from observations in the visual and near ultraviolet spectra ranges. Their investigation yielded metal deficiencies of up to 1.0 dex; iron was found to be underabundant by 0.60 dex, if a solar iron abundance of $\varepsilon(\text{Fe}) = 7.51$ is assumed.
14. Desikachary & Hearnshaw (1982) have taken a weighted mean of seven determinations from Johnson and Strömgren photometry, absolute spectrophotometry, intensity interferometry and infrared fluxes. The surface gravity was provided by fits to the $\text{H}\gamma$ and $\text{H}\delta$ -line profiles as well as to Strömgren ($b - y$) and c_1 indices. Luck & Lambert (1985) quoted that using their parameters ($T_{\text{eff}} = 7500\text{K}$ and $\log g = 1.5$) reproduces the observed Balmer line profiles about as well as Desikachary and Hearnshaw's alternative pairing of $T_{\text{eff}} = 7350\text{K}$ and $\log g = 1.8$. Four échelle spectrograms were obtained with a resolution varying between 0.07Å and 0.10Å . The microturbulent velocity was measured from 33 Fe I lines on the saturated part of the curve of growth ($-5.0 \leq \log(W/\lambda) \leq -4.40$). No evidence for depth-dependence of the microturbulence was found in Canopus. The model atmosphere grid computed by Kurucz (1979) was used for this analysis. Hydrostatic and ionisation equilibrium equations are solved and the line formation problem in LTE is treated to obtain the equivalent widths of lines of a given element and hence the abundance.
15. Lambert et al. (1982) have obtained carbon, nitrogen, and oxygen abundances from C I, N I and O I high-excitation permitted lines. These results are based on model atmospheres and observed spectra. The effective temperature and gravity found by Dreiling & Bell (1980) and Bell & Dreiling (1981) were used to independently determine the metallicity and microturbulent velocity.
16. Boyarchuk & Lyubimkov (1983) have used published high-dispersion spectroscopic data in order to analyse Canopus. The effective temperature and gravity are determined by using the Balmer lines $\text{H}\gamma$ and $\text{H}\delta$, the energy distribution in the continuum and the ionisation equilibrium for V, Cr and Fe. Using the Fe I lines yields a microturbulence of 4.5 km s^{-1} , while a microturbulence of 6.0 km s^{-1} was derived from the Ti II, Fe II and Cr II lines. At that moment, Boyarchuk and Lyubimkov could not explain this phenomenon, but later on, in 1983, Boyarchuk and Lyubimkov could explain this as being due to non-LTE effects.
17. Lyubimkov & Boyarchuk (1984) have used the model found by Boyarchuk & Lyubimkov (1983) to determine the abundances of 21 elements in the atmosphere of Canopus. The microturbulence derived from the Fe I lines was used. By comparison with evolutionary calculations, the mass, radius, luminosity, and age are found. It is demonstrated that the extension of the atmosphere is small compared to the radius.
18. Luck & Lambert (1985) have acquired data for Canopus with the ESO Coudé auxiliary telescope and Reticon equipped echelle spectrograph, with a resolution of 0.05Å . The equivalent widths were determined by direct integration of the line profiles. Both photometry and a spectroscopic analysis are used for the determination of the atmospheric parameters. Broad- (*UBVRIJK*) and narrow- (*uvby*) band photometry were available for Canopus. Using different colour-temperature relations, T_{eff} and $\log g$ were determined in different ways. The uncertainties in these (photometric) values are estimated to be $\pm 50\text{K}$ in T_{eff} and $\pm 0.2\text{ dex}$ in $\log g$. Spectroscopic estimates of T_{eff} , $\log g$ and ξ_t are proceeded using the classical requirements: (1) T_{eff} is set by requiring that the individual abundances from the Fe I lines are independent of the lower excitation potential; (2) the requirement that the individual abundances of the Fe I lines show no dependence on line strength provides ξ_t ; (3) $\log g$ is determined by forcing the Fe I and Fe II lines to give the same abundance. The formal uncertainties in spectroscopic parameter determinations are typically $\pm 200\text{K}$ in T_{eff} , $\pm 0.3\text{ dex}$ in $\log g$ and $\pm 0.5\text{ km s}^{-1}$ in ξ_t . Although various attempts have been performed, the scatter on the iron abundance determined from the Fe I lines remained quite high (0.26 dex). The photometric values of T_{eff} range from 7320 to 7900 K, with the spectroscopic value being 7500 K. From the ($b - y/c_1$) colour, a surface gravity of 1.80 is ascertained, while the spectroscopic determination yields a value of 1.50. Finally, the abundances for C, N, and O have been determined by spectrum synthesis using the spectroscopic atmospheric values, with the N abundance being computed from a non-LTE analysis. They quoted that the N-abundance of Desikachary & Hearnshaw (1982) is rather uncertain due to their LTE analysis and the use of blended or very weak lines. Although Luck & Lambert (1985) have performed a non-LTE analysis to determine $\varepsilon(\text{N})$, they do not have taken NLTE-effects into account in the determination of the spectroscopic atmospheric parameters.
19. Moon (1985) has found a linear relation between the visual surface brightness parameter F_v and the ($b - y$)₀ colour index of *uvby* β photometry for spectral types later than G0. Using this relation, tables of intrinsic

- colours and indices, absolute magnitude and stellar radius are given for the ZAMS and luminosity classes Ia - V over a wide range of spectral types.
20. From empirically calibrated *uvby* β grids, Moon & Dworetzky (1985) have determined the effective temperature and surface gravity of a sample of stars. The authors divided the temperature range into three region ($T_{\text{eff}} \leq 8500\text{K}$, $T_{\text{eff}} \geq 11000\text{K}$ and the region in between these two temperature values) and have given for every region one grid. Comparison with fundamental measurements of T_{eff} and $\log g$ (Code et al. 1976) shows an excellent agreement, while Balona's formula (Balona 1984) for B stars gives values with a mean difference of $110 \pm 360\text{K}$ for the temperature and $0.22 \pm 0.15\text{dex}$ for the gravity. A program for the analysis of photometric data based on these grids has been presented by Moon & Dworetzky (1985). Napiwotzki et al. (1993) quoted however that they have noted discrepancies between the values of T_{eff} and $\log g$ derived from the published grid and the values derived from the polynomial fits used in the program of Moon & Dworetzky (1985). Therefore Napiwotzki et al. (1993) have completely rewritten this program.
 21. Using the absolute parallax and the observed apparent magnitudes, Demarque et al. (1986) have calculated the absolute magnitudes and masses for the components of α Cen A and α Cen B.
 22. Based on high-dispersion spectra covering the wavelength range 3050 – 6850 Å, a model-atmosphere analysis of the Fe I/Fe II spectrum of Vega has been carried out by Gigas (1986) taking into account departures from LTE. The parameters $T_{\text{eff}} = 9500\text{K}$ and $\log g = 3.9$ derived by Lane & Lester (1984) have been adopted. The microturbulence has been derived in the usual way by varying ξ_t until all iron lines yielded (almost) the same metal abundance independent of the equivalent width. After various test calculations it has been found that the best fit is given by a microturbulent velocity decreasing with optical depth.
 23. Lester et al. (1986) have performed a calibration of the effective temperature and gravity using the Strömgen *uvby* β indices based on the line-blanketed LTE stellar atmospheres from Kurucz (1979). The indices have been placed on the standard systems using the ultraviolet and visual energy distributions of the secondary spectrophotometric standards. For these standard stars, the effective temperature and surface gravity have been determined by finding the model atmosphere which best matched the observed visual and ultraviolet energy distribution. They have shown that the common practice of using a single standard star to effect the transformation of the computed indices to the standard system produces systematic errors.
 24. From a limited set of high-quality data, Smith & Lambert (1986) have determined the physical parameters of α Cen A and α Cen B. Therefore a conventional analysis based on LTE model atmospheres derived from the Holweger-Müller solar atmosphere has been used. From the data they have constructed a series of logarithmic abundance against effective temperature diagrams, each diagram corresponding to fixed values of microturbulence and surface gravity. The region or 'neck' where these lines converge indicates the values of the effective temperature and the metallicity.
 25. Soderblom (1986) has compared high-resolution and high signal-to-noise observations of H α in the Sun, α Cen A and α Cen B to models in order to derive temperatures. These temperatures were then used to calculate the radii of these stars from the luminosity values given by Flannery & Ayres (1978).
 26. di Benedetto & Rabbia (1987) used Michelson interferometry by the two-telescope baseline located at CERGA. Combining this angular diameter with the bolometric flux F_{bol} (resulting from a directed integration using the trapezoidal rule over the flux distribution curves, after taking interstellar absorption into account) they found the effective temperature, which was in good agreement with results obtained from the lunar occultation technique. di Benedetto (1998) calibrated the surface brightness-colour correlation using a set of high-precision angular diameters measured by modern interferometric techniques. The stellar sizes predicted by this correlation were then combined with bolometric-flux measurements, in order to determine one-dimensional (T , $V - K$) temperature scales of dwarfs and giants. Both measured and predicted values for the angular diameter are listed.
 27. Abia et al. (1988) have obtained high-resolution, high signal-to-noise spectra of 23 disk stars. Values for the effective temperature were derived from photometric indices ($b - y$) and ($R - I$). The mean of these values, given by these two photometric indices, was used as effective temperature. For α Cen A, the value given by Soderblom (1986) was used. The $\log g$ values were derived from the ($b - y$) and c_1 indices. A microturbulence parameter of 1.5 km s^{-1} was adopted for all the stars for which the value was not found in the literature. Two parallel approaches were used to determine the abundances: method (a) in which the equivalent width of lines were fitted to curves of growth derived from the model atmosphere adopted for each star, and method (b) in which the synthetic spectra were fitted to the observed lines by interactive fitting using a high-resolution graphics terminal. In no case did the two methods disagree by more than 0.03 dex in the derived abundances.
 28. Edvardsson (1988) determined logarithmic surface gravities from the analysis of pressure broadened wings of strong metal lines. Comparisons with trigonometrically determined surface gravities give support to the spectroscopic results. Surface gravities determined from the ionisation equilibria of Fe and Si are found to be systematically lower than the strong line gravities, which may be an effect of errors in the model atmospheres, or departures from LTE in the ionisation equilibria. When the effective temperature of α Cen A

derived by Smith et al. (1986) would be used, instead of the used 5750 K, the deduced gravity should only change by an amount $\leq +0.04$ dex.

29. Fracassini et al. (1988) have made a catalogue of stellar apparent diameters and/or absolute radii, listing 12055 diameters for 7255 stars. Only the most extreme values are listed. References and remarks to the different values of the angular diameter and radius may be found in this catalogue. Also here these angular diameter values are given in italic mode when determined from direct methods and in normal mode for indirect (spectrophotometric) determinations.
30. Russell & Bessell (1989) have derived initial estimates for the physical parameters of their programme stars from photometry in the medium-bandwidth *ubvy* Strömgren system. For Canopus the physical parameters derived by Boyarchuk & Lyubimkov (1983) were then used ($T_{\text{eff}} = 7400$ K, $\log g = 1.9$) to derive the abundances from spectroscopic observations made with the 1.88m telescope in Canberra. Therefore the analysis program WIDTH6 — a derivative of Kurucz's ATLAS5 code (Kurucz 1970), using the classical assumptions of LTE, hydrostatic equilibrium and a plane-parallel atmosphere — was used. The mass was derived from evolutionary models and the absolute visual magnitude has been determined from the observed, visual magnitude, the visual interstellar extinction and the distance modulus. Using the bolometric corrections, the bolometric magnitude has been determined, which then yields, in conjunction with the effective temperature, the radius of the star.
31. Sadakane & Ueta (1989) have analysed the high-resolution spectral atlas of Sirius published by Kurucz & Furenlid (1979). Using as effective temperature $T_{\text{eff}} = 10000$ K and surface gravity $\log g = 4.30$ the abundances of 19 ions were determined by use of the WIDTH6 program of Kurucz. By requiring that the abundance is independent of the equivalent width, the microturbulence was obtained.
32. Spite et al. (1989) have used an ESO-CES spectrograph spectrum of Canopus. The temperature was adopted from Luck & Lambert (1985). The surface gravity was determined by forcing the Fe I and the Fe II lines to yield the same abundance. The microturbulence was derived from the Fe I lines and was assumed to apply to all species. Using these parameters the metallicity was ascertained.
33. Volk & Cohen (1989) determined the effective temperature directly from the literature values of angular-diameter measurements and total-flux observations (also from literature). The distance was taken from the Catalog of Nearby Stars (Gliese 1969) or from the Bright Star Catalogue (Hoffleit & Jaschek 1982).
34. An elemental abundance analysis of Vega has been performed by Adelman & Gulliver (1990) using high signal-to-noise 2.4 \AA mm^{-1} Reticon observations of the region $\lambda\lambda 4313 - 4809$. The effective temperature and surface gravity were adopted from Kurucz (1979). The program WIDTH6 of Kurucz (1993) was used to deduce the abundances of metal lines from the measured equivalent widths and adopted model atmospheres. The adopted value for the microturbulence is the mean of all the Fe I and Fe II values.
35. Furenlid & Meylan (1990) have used high-dispersion Reticon spectra to perform a differential analysis between the Sun and α Cen. The model atmosphere analysis was carried out using the WIDTH6 program by Kurucz. The program was used in an iterative mode, where abundances, effective temperature, surface gravity and microturbulence are treated as free parameters, and the measured equivalent-width values together with the appropriate atomic constants are the fixed input parameters. Four specific criteria define a consistent solution: the derived abundances must be independent of (1) the excitation potential of the lines; (2) the equivalent-width values of the lines; (3) the optical depth of formation of the lines; and (4) the level of ionisation of elements with lines in more than one stage of ionisation.
36. Based on high-resolution Reticon spectra Lemke (1990) has derived abundances of C, Si, Ca, Sr, and Ba for 16 sharp lined, main sequence A stars. Strömgren photometry was converted into effective temperature and gravity by means of the calibration of Moon & Dworetzky (1985). From these parameters, model atmospheres were computed with the ATLAS6 code of Kurucz. Equivalent widths were measured by direct integration of the data. A program computed the quantity $\log gf\varepsilon$ in such a way that computed and observed equivalent widths agree. Optionally, NLTE departure coefficients for calcium and barium could be taken into account.
37. Malagnini & Morossi (1990) have used spectrophotometric data (in the wavelength range from 3200 Å to 10000 Å) and trigonometric parallaxes to determine the stellar parameters. Using the Kurucz (1979) models, they have performed a fitting procedure which permits to obtain, simultaneously, accurate estimates not only of the effective temperature and apparent angular diameter, but also for the $E(B - V)$ excess for $T_{\text{eff}} > 9000$ K. From the angular diameter and the parallax, the stellar radius is computed and so the luminosity is determined. To derive the mass and the surface gravity, they have compared the stellar position in the H-R diagram with theoretical evolutionary tracks. An uncertainty of 0.15 dex is derived for $\log g$. By taking into account contributions from different sources to the total error, the average uncertainty affecting the stellar effective temperature, radius, and luminosity is on the order of 2%, 16% and, 35% respectively.
38. McWilliam (1990) based his results on high-resolution spectroscopic observations with resolving power 40000. The effective temperature was determined from empirical and semi-empirical results found in the literature and from broad-band Johnson colours. The gravity was ascertained by using the well-known relation between g ,

- T_{eff} , the mass M and the luminosity L , where the mass was determined by locating the stars on theoretical evolutionary tracks. So, the computed gravity is fairly insensitive to errors in the adopted L . High-excitation iron lines were used for the metallicity $[\text{Fe}/\text{H}]$, in order that the results are less spoiled by non-LTE effects. The author refrained from determining the gravity in a spectroscopic way (i.e. by requiring that the abundance of neutral and ionised species yields the same abundance) because ‘*A gravity adopted by demanding that neutral and ionised lines give the same abundance, is known to yield temperatures which are ~ 200 K higher than found by other methods. This difference is thought to be due to non-LTE effects in Fe I lines.*’. By requiring that the derived iron abundance, relative to the standard 72 Cyg, were independent of the equivalent width of the iron lines, the microturbulent velocity ξ_t was found.
39. Venn & Lambert (1990) have determined the chemical composition of three λ Bootis stars and the “normal” A star Vega. Equivalent widths derived from the spectra — obtained using the Reticon camera at the coude focus of the 2.7 m telescope at the McDonald Observatory — were converted to abundances using the program WIDTH6 (Kurucz 1993). The effective temperature and gravity found from a detailed study by Dreiling & Bell (1980) have been adopted. For the microturbulent velocity, they used the value of 2 km s^{-1} of Lambert et al. (1982).
 40. Achmad et al. (1991) used several sets of equivalent widths available in the literature. More than 2000 lines are then used in a least-square iterative routine in which T_{eff} , $\log g$, ξ_t and $[\text{Fe}/\text{H}]$ are determined simultaneously. The results are compared with those of other authors. No significant variation of ξ_t with depth is found.
 41. Chmielewski et al. (1992) have used Reticon spectrograms of α Cen A and α Cen B to determine their stellar parameters. Like demonstrated by Cayrel et al. (1985) the wings of the hydrogen H_α line profile can be used to provide the effective temperature relative to the sun. Using the mass found by Demarque et al. (1986), the gravity was calculated from the effective temperature, the mass, the visual magnitude and the bolometric correction. A microturbulent velocity parameter of 1 km s^{-1} was adopted. Using a curve of growth the iron and nickel abundances were determined.
 42. Engelke (1992) has derived a two-parameter analytical expression approximating the long-wavelength ($2 - 60 \mu\text{m}$) infrared continuum of stellar calibration standards. This generalised result is written in the form of a Planck function with a brightness temperature that is a function of both observing wavelength and effective temperature. This function is then fitted to the best empirical flux data available, providing thus the effective temperature and the angular diameter.
 43. Pottasch et al. (1992) reported on the detection of solar-like p-modes of oscillation with a period near 5 minutes on α Cen. Using this result, the radius is derived, which gives, in conjunction with the effective temperature, the stellar luminosity.
 44. Hill & Landstreet (1993) have used spectra obtained with the coude spectrograph of the Dominion Astrophysical Observatory 1.2 m telescope. The parameters for the model atmospheres for the spectrum synthesis were chosen using *wby*H β photometry. As error bars on these atmospheric parameters the values as derived by Lemke (1990) were taken. The model atmospheres were then obtained by interpolating in T_{eff} and $\log g$ within the grid of plane-parallel, line-blanketed, LTE model atmospheres published by Kurucz (1979). These atmospheres assume a depth-independent microturbulence of 2 km s^{-1} and a solar composition. The spectrum synthesis is performed by a new program, which searches for the values of the microturbulence, the radial velocity, $v \sin i$, and selected abundances by minimising the mean square difference between the observed and synthetic spectrum.
 45. Napiwotzki et al. (1993) have performed a critical examination of the determination of stellar temperatures and surface gravity by means of the Strömngren *wby* β photometric system in the region of main-sequence stars. In particular, the calibrations of Moon & Dworetzky (1985), Lester et al. (1986) and Balona (1984) are discussed. For the selection of temperature standards, only those stars were included for which an integrated-flux temperature was available. The temperatures had to be based on measurements of the absolute integrated flux which include both the visual and ultraviolet region. The angular diameter had to be determined by using the V magnitude or by using the method proposed by Malagnini et al. (1986), who fitted model spectra to observed spectra by varying T_{eff} , $\log g$ and θ_d . Results from the IRFM method were excluded due to systematic errors which seem to destroy the reliability of the results obtained by the IRFM method. Napiwotzki et al. (1993) quoted that the resulting IRFM temperatures are too low by 1.6 – 2.8%, corresponding to angular diameters which are too large by 3.5 – 5.9%. In the tables with literature values for β Leo and Vega the mean value of the quoted integrate-flux temperatures is listed. The photometric temperature values are then checked against the integrate-flux temperature values. For the gravity calibration, the authors have determined the surface gravity by fitting theoretical profiles of hydrogen Balmer lines (Kurucz 1979) to the observations. These spectroscopic gravities were then compared with gravities derived from photometric calibrations. From their results, they recommended the Moon and Dworetzky calibration, if corrected for gravity deviation. The final statistical error of the temperature determination ranges from 2.5% for stars with $T_{\text{eff}} \leq 11000 \text{ K}$ up to 4% for $T_{\text{eff}} \geq 20000 \text{ K}$, while the accuracy for the gravity determinations ranges from ~ 0.10 dex for early A stars to ~ 0.25 dex for hot B stars.

46. Popper (1993) has determined the masses of G – K main-sequence stars by observations of detached eclipsing binaries of short period with the CCD-echelle spectrometer. A mass of $1.14 M_{\odot}$ was found for α Cen A, which results in a gravity of $\log g = 4.3$ when a radius-value found in the literature is used.
47. Smalley & Dworetzky (1993) have presented a detailed investigation into the methods of determining the atmospheric parameters of stars in the spectral range A3 – F5. A comparison is made between atmospheric parameters derived from Strömngren *uvby* β photometry, from spectrophotometry, and from Balmer line profiles. The photometric results found by Relyea & Kurucz (1978), Moon & Dworetzky (1985), Lester et al. (1986), and Kurucz (1991) are confronted with each other. All the various photometric calibrations give generally the same T_{eff} and $\log g$ to within ± 200 K and ± 0.2 dex respectively. The model m_0 colours (which are sensitive to the metal abundance) do however not adequately reproduce the observed values due to inadequacies in the opacities of the Kurucz (1979) models. Another reason for poorer results of any of the existing grids of model atmospheres to reproduce m_0 is the fact that this index is also quite sensitive to the onset of convection which affects any prediction of m_0 for stars later than about A5. Experiments with different treatments of convection point towards convection as the remaining major source of uncertainty for the determination of fundamental parameters from photometric calibrations using model atmospheres in this temperature region of the HR diagram (Smalley & Kupka 1997). By fitting optical and ultraviolet spectrophotometric fluxes, the authors have derived the values of T_{eff} and $\log g$. These spectroscopic values for T_{eff} and $\log g$, corresponding to two different metallicities, are the first two values listed for β Leo. Using the new Kurucz (1991) model fluxes instead of the Kurucz (1979) model fluxes, yields T_{eff} -values which differ by only ± 100 K, but the gravity is higher by typically 0.2 – 0.3 dex. The obtained spectrophotometric values for T_{eff} and $\log g$ are in good agreement with the results from the *uvby* β photometry, but are systematically lower than the spectrophotometric T_{eff} and $\log g$ given by Lane & Lester (1984). The reason for this discrepancy was found to be an insufficient allowance for the metal abundance by Lane & Lester (1984). A third method was based on medium-resolution spectra of H β and H γ line profiles in order to obtain the T_{eff} for the 52 A and F stars. These results for two different metallicities are the last two values listed for β Leo. These results are in good agreement with the photometric T_{eff} and $\log g$ values. The authors have concluded that the values of T_{eff} and $\log g$ determined from photometry are extremely reliable and not significantly affected by the metallicity.
48. The abundances of five iron-peak elements (chromium through nickel) are derived by Smith & Dworetzky (1993) by spectrum-synthesis analysis of co-added high-resolution IUE spectra. The effective temperature and gravity were derived from calibrations of Strömngren and Geneva photometric systems based on spectroscopically normal stars and solar-metallicity model atmospheres. Further constraints on the effective temperature and surface gravity of the programme stars were obtained by fitting the predictions of Kurucz (1979) solar-metallicity model atmospheres to de-reddened spectrophotometric scans and H γ profiles of the programme stars taken primarily from the literature. The adopted atmospheric parameters are mean values from the photometric and ‘best-fit’ spectroscopic analyses. The microturbulence parameter was taken from fine analyses of visual-region spectra in the literature. Elemental abundances were then determined by interactively fitting the observations with LTE synthetic spectra computed using the Kurucz (1979) models.
49. Castelli & Kurucz (1994) have compared blanketed LTE models for Vega computed both with the opacity distribution function method and the opacity-sampling method. The stellar parameters (T_{eff} , $\log g$ and [Fe/H]) were fixed by comparing the observed ultraviolet, visual, and near infrared flux with the computed one and by comparing observed and computed Balmer profiles. A microturbulent velocity of 2 km s^{-1} was assumed. The model parameters for Vega depend on the amount of reddening and on the helium abundance.
50. The effective temperature, surface gravity and mass of Harris & Lambert (1984) were used by El Eid (1994). He noted a correlation between the $^{16}\text{O}/^{17}\text{O}$ ratio and the stellar mass and the $^{12}\text{C}/^{13}\text{C}$ ratio and the stellar mass for evolved stars. Using this ratio in conjunction with evolutionary tracks, El Eid has determined the mass.
51. Gadun (1994) has used model parameters and equivalent widths of Fe I and Fe II lines for α Cen, α Boo, and α Car found in literature. It turned out that the Fe I lines were very sensitive to the temperature structure of the model and that iron was over-ionised relative to the LTE approximation due to the near-ultraviolet excess $J_{\nu} - B_{\nu}$. Since the concentration of the Fe II ions is significantly higher than the concentration of the neutral iron atoms, the iron abundance was finally determined using these Fe II lines. It is demonstrated that there is a significant difference in behaviour of ξ_t from the Fe I lines for solar-type stars, giants, and supergiants. The microturbulent velocity decreases in the upper photospheric layers of solar-type stars, in the photosphere of giants (like Arcturus) ξ_t has the tendency to increase and in Canopus, a supergiant, a drastic growth of ξ_t is seen. This is due to the combined effect of convective motions and waves which form the base of the small-scale velocity field. The velocity of convective motions decreases in the photospheric layers of dwarfs and giants, while the velocity of waves increases due to the decreasing density. In solar-type stars the convective motion penetrates in the line-forming region, while the behaviour of ξ_t in Canopus may be explained by the

- influence of gravity waves. The characteristics of the microturbulence determined from the Fe II lines differ from that found with Fe I lines. These results can be explained by 3D numerical modelling of the convective motions in stellar atmospheres, where it is shown that the effect of the lower gravity is noticeable in the growth of horizontal velocities above the stellar ‘surface’ (in the region of Fe I line formation). But in the Fe II line-forming layers the velocity fields are approximately equal in 3D model atmospheres with a different surface gravity and same T_{eff} . Both values for ξ_t derived from the Fe I and Fe II lines are listed. If the microturbulence varies, the values of ξ_t are given going outward in the photosphere.
52. Hill et al. (1995) have taken the equivalent widths for Canopus from Desikachary & Hearnshaw (1982), Luck & Lambert (1985) and Spite et al. (1989). As a first approach, the effective temperature was estimated from a $(B - V)$ - T_{eff} calibration. This first guess for the temperature was checked, when possible, by fitting the observed and computed profiles of the $H\alpha$ wings. The final T_{eff} -values were determined by requiring the Fe I abundances to be independent of the excitation potential of the lines. The formal uncertainty in this determination is about ± 200 K. The surface gravity was adjusted to obtain the same iron abundance from weak Fe I and Fe II lines. This gives a maximum uncertainty of 0.3 dex on the gravity. The microturbulent velocity was determined by requiring the abundances derived from the Fe I lines to be independent of the line’s equivalent width. The uncertainty on ξ_t is of the order of 0.5 km s^{-1} . By varying these three stellar parameters, it was seen that no dramatic changes appear upon gravity and microturbulence variation. Significant changes in $[\text{Fe}/\text{H}]$ values take place as a result of temperature variation, but the relative elemental abundances are changed negligibly. The error in abundances is of the order of ± 0.1 dex to ± 0.2 dex, but the error in abundances relative to iron only ranges from ± 0.01 dex to ± 0.1 dex, depending on the element. The errors listed in Table 3 for α Car are the *intrinsic* errors. Taking into account the overionisation due to NLTE-effects, yields for a star with similar atmospheric parameters the same temperature, but an increase in gravity and ξ_t . Model atmospheres were interpolated in a grid using the MARCS-code of Gustafsson et al. (1975).
 53. Holweger & Rentzsch-Holm (1995) have included β Leo in their sample of normal main-sequence B9.5 – A6 stars whose infrared excess indicates the presence of a circumstellar dust disk. Using published Strömgren photometry and the calibration of Napiwotzki et al. (1993) the temperature and surface gravity was determined. The error-bars are the ones quoted by Napiwotzki et al. (1993).
 54. Smalley & Dworetzky (1995) have presented an investigation into the determination of fundamental values of T_{eff} and $\log g$. Using angular diameters of Brown et al. (1974) and ultraviolet and optical fluxes, the effective temperature was derived. For stars in eclipsing and visual binary systems, fundamental values for the gravity were listed. For stars with $T_{\text{eff}} > 8500$ K, fits were also made to the $H\beta$ profiles to determine $\log g$. The Strömgren-Crawford $uvby\beta$ photometric system provided a quick and efficient mean of estimating the atmospheric parameters of B, A, and F stars. Therefore several model atmosphere calibrations were available.
 55. Sokolov (1995) has used the slope of the Balmer continuum between 3200 \AA and 3600 \AA in order to determine the effective temperature of B, A, and F main-sequence stars. Therefore, stars were selected from two catalogues of low-resolution spectra, observed in the wavelength region from 3100 \AA to 7400 \AA with a step of 25 \AA . Based on a selection of temperature standards found in different literature sources, the author has determined the relationship between T_{eff} and the slope of the Balmer continuum. The effective temperatures determined in that way are in good agreement with results found by other authors using different methods. The statistical errors of the temperature determination range from 4 % for stars with $T_{\text{eff}} \leq 10000$ K up to 10 % for stars with $T_{\text{eff}} \geq 20000$ K.
 56. Hui-Bon-Hoa et al. (1997) have investigated 11 A stars in young open clusters and three field stars by means of high-resolution spectroscopy. The effective temperature and surface gravity were determined by using the $uvby\beta$ photometry and the grids of Moon & Dworetzky (1985). The model atmosphere is then interpolated in the grids of Kurucz’ ATLAS9 models (Kurucz 1993). The microturbulent velocity is obtained by the constraint that all the lines of a same element should yield the same abundance.
 57. Malagnini & Morossi (1997) have discussed the uncertainties affecting the determinations of effective temperature and apparent angular diameters based on the flux fitting method. Therefore they have analysed the influence of the indetermination of some fixed secondary parameters (i.e. surface gravity, overall metallicity and interstellar reddening) on the estimates of the fitted parameters T_{eff} and θ_d . A database of visual spectrophotometric data together with a grid of theoretical models of Kurucz (1993) is used. By varying the fixed parameters, being $\log g$, $[\text{M}/\text{H}]$ and $E(B - V)$, by ± 0.5 , ± 0.5 dex and ± 0.02 mag respectively, the uncertainties in the determinations of T_{eff} and θ_d are found to be of the order of 2 % (median values) spanning ranges 0.6 – 5.3 % and 1 – 9 % respectively. The authors concluded that these uncertainties must be taken into account by those scientists who use the effective temperatures, based on the flux fitting method, in their analysis of high-resolution spectra in order to avoid systematic errors in their results on chemical abundances of individual elements.
 58. Neuforge-Verheecke & Magain (1997) have performed a detailed spectroscopic analysis of the two components of the binary system α Centauri on the basis of high-resolution and high signal-to-noise spectra. The tem-

peratures of the stars have been determined from the Fe I excitation equilibrium and checked from the H α line wings. In each star, the microturbulent velocity, ξ_t , is determined so that the abundances derived from the Fe I lines are independent of their equivalent widths and the surface gravity is ascertained by forcing the Fe II lines to indicate the same abundance as the Fe I lines. The abundances are adjusted until the calculated equivalent width of a line is equal to the observed one.

59. Rentzsch-Holm (1997) has determined nitrogen and sulphur abundances in 15 sharp-lined ‘normal’ main sequence A stars from high-resolution spectra obtained with the Coudé spectrograph (CES) of the ESO 1.4 m telescope. Stellar parameters were adopted from Lemke (1990). Using the ATLAS9 model atmospheres of Kurucz (1993), detailed non-LTE calculations are performed for each model atmosphere.
60. di Benedetto (1998) calibrated the surface brightness-colour correlation using a set of high-precision angular diameters measured by modern interferometric techniques. The stellar sizes predicted by this correlation were then combined with bolometric-flux measurements, in order to determine one-dimensional (T , $V - K$) temperature scales of dwarfs and giants. Both measured and predicted values for the angular diameter are listed.
61. Using Strömgren photometry, Gardiner et al. (1999) estimated β Leo to be slightly overabundant, $[\text{Fe}/\text{H}] = +0.2$ dex. From their research, one may conclude that the determination of the effective temperature and gravity for β Leo from Balmer line profiles (as done by Smalley & Dworetzky 1995) seems to be rather uncertain, since β Leo is located close to the maximum of the Balmer line width as a function of the effective temperature and the Balmer lines are very sensitive to $\log g$ in this region.
62. Instead of disjoint determinations of the visual orbit, the mass ratio and the parallax, Pourbaix et al. (1999) have undertaken a simultaneous adjustment of all visual and spectroscopic observations for α Cen. This yielded for the first time an agreement between the astrometric and spectroscopic mass ratio. The orbital parallax differs from all previous estimates, the Hipparcos one being the closest to their value.
63. Near-infrared ($2.2 \mu\text{m}$) long baseline interferometric observations of Vega are presented by Ciardi et al. (2001). The stellar disk of the star has been resolved and the limb-darkened stellar diameter and the effective temperature are derived. The derived value for the angular diameter agrees well with the value determined by Brown et al. (1974), $\theta_d = 3.24 \pm 0.07$ mas.
64. On the basis of high-resolution echelle spectra obtained with the Coudé Echelle Spectrograph attached to the 2.16 m telescope at the Beijing Astronomical Observatory Qiu et al. (2001) have performed an elemental abundance analysis of Sirius and Vega. For the effective temperature, they adopted the values obtained by Moon & Dworetzky (1985) based on $uvby\beta$

photometry. The empirical method to determine the surface gravity by requiring that Fe I and Fe II give the same abundance has been employed. The microturbulence has been derived in the usual way by requiring that all the iron lines yield the same abundance independent of the line strength. Usually, they have taken the initial model metallicity from previous published analyses. They then have iterated the whole procedure to give the convergence value to be the model overall metallicity. Model atmospheres generated by the ATLAS9 code (Kurucz 1993) were used in the abundance analysis. The resulting abundance pattern was then compared with other published values.

References

- Abia, C., Rebolo, R., Beckman, J. E., & Crivellari, L. 1988, *A&A*, 206, 100
- Achmad, L., de Jager, C., & Nieuwenhuijzen, H. 1991, *A&A*, 249, 192
- Adelman, S. J. & Gulliver, A. F. 1990, *ApJ*, 348, 712
- Balona, L. A. 1984, *MNRAS*, 211, 973
- Bell, R. A. & Dreiling, L. A. 1981, *ApJ*, 248, 1031
- Blackwell, D. E., Petford, A. D., & Shallis, M. J. 1980, *A&A*, 82, 249
- Blackwell, D. E. & Shallis, M. J. 1977, *MNRAS*, 180, 177
- Boyarchuk, A. A. & Lyubimkov, L. S. 1983, *Astrophysics*, 18, 228
- Brown, R. H., Davis, J., & Allen, L. R. 1974, *MNRAS*, 167, 121
- Castelli, F. & Kurucz, R. L. 1994, *A&A*, 281, 817
- Cayrel, R., Cayrel de Strobel, G., & Campbell, B. 1985, *A&A*, 146, 249
- Chmielewski, Y., Friel, E., Cayrel de Strobel, G., & Bentolila, C. 1992, *A&A*, 263, 219
- Ciardi, D. R., van Belle, G. T., Akeson, R. L., et al. 2001, *ApJ*, 559, 1147
- Code, A. D., Bless, R. C., Davis, J., & Brown, R. H. 1976, *ApJ*, 203, 417
- Decin, L., Vandenbussche, B., Waelkens, C., et al. 2002, *A&A*, in press, (Paper II)
- Demarque, P., Guenther, D. B., & van Altena, W. F. 1986, *ApJ*, 300, 773
- Desikachary, K. & Hearnshaw, J. B. 1982, *MNRAS*, 201, 707
- di Benedetto, G. P. 1998, *A&A*, 339, 858
- di Benedetto, G. P. & Rabbia, Y. 1987, *A&A*, 188, 114
- Dreiling, L. A. & Bell, R. A. 1980, *ApJ*, 241, 736
- Edvardsson, B. 1988, *A&A*, 190, 148
- El Eid, M. F. 1994, *A&A*, 285, 915
- Engelke, C. W. 1992, *AJ*, 104, 1248
- England, M. N. 1980, *MNRAS*, 191, 23
- Flannery, B. P. & Ayres, T. R. 1978, *ApJ*, 221, 175
- Fracassini, M., Pasinetti-Fracassini, L. E., Pastori, L., & Pironi, R. 1988, *Bulletin d’Information du Centre de Donnees Stellaires*, 35, 121
- Furenlid, I. & Meylan, T. 1990, *ApJ*, 350, 827
- Gadun, A. S. 1994, *Astronomische Nachrichten*, 315, 413

- Gardiner, R. B., Kupka, F., & Smalley, B. 1999, *A&A*, 347, 876
- Gigas, D. 1986, *A&A*, 165, 170
- Gliese, W. 1969, *Veröffentlichungen des Astronomischen Rechen-Instituts Heidelberg*, 22, 1
- Gustafsson, B., Bell, R. A., Eriksson, K., & Nordlund, Å. 1975, *A&A*, 42, 407
- Harris, M. J. & Lambert, D. L. 1984, *ApJ*, 285, 674
- Hill, G. M. & Landstreet, J. D. 1993, *A&A*, 276, 142
- Hill, V., Andrievsky, S., & Spite, M. 1995, *A&A*, 293, 347
- Hoffleit, D. & Jaschek, C. 1982, *The Bright Star Catalogue (The Bright Star Catalogue, New Haven: Yale University Observatory (4th edition), 1982)*
- Holweger, H. & Rentzsch-Holm, I. 1995, *A&A*, 303, 819
- Hui-Bon-Hoa, A., Burkhart, C., & Alecian, G. 1997, *A&A*, 323, 901
- Kamper, K. W. & Wesselink, A. J. 1978, *AJ*, 83, 1653
- Kurucz, R. 1993, *ATLAS9 Stellar Atmosphere Programs and 2 km/s grid. Kurucz CD-ROM No. 13. Cambridge, MA: Smithsonian Astrophysical Observatory*
- Kurucz, R. L. 1970, *SAO Special Report*, 308
- . 1979, *ApJS*, 40, 1
- Kurucz, R. L. 1991, in *Stellar Atmospheres: Beyond Classical Models, Proceedings of the Advanced Research Workshop.*, 441
- Kurucz, R. L. & Furenlid, I. 1979, *Smithsonian Astrophys. Obs. Spec. Rept.*, 387
- Lambert, D. L., Roby, S. W., & Bell, R. A. 1982, *ApJ*, 254, 663
- Lane, M. C. & Lester, J. B. 1984, *ApJ*, 281, 723
- Lemke, M. 1990, *A&A*, 240, 331
- Lester, J. B., Gray, R. O., & Kurucz, R. L. 1986, *ApJS*, 61, 509
- Linsky, J. L. & Ayres, T. R. 1978, *ApJ*, 220, 619
- Luck, R. E. 1979, *ApJ*, 232, 797
- Luck, R. E. & Lambert, D. L. 1985, *ApJ*, 298, 782
- Lyubimkov, L. S. & Boyarchuk, A. A. 1984, *Astrophysics*, 19, 385
- Malagnini, M. L. & Morossi, C. 1990, *A&AS*, 85, 1015
- . 1997, *A&A*, 326, 736
- Malagnini, M. L., Morossi, C., Rossi, L., & Kurucz, R. L. 1986, *A&A*, 162, 140
- McWilliam, A. 1990, *ApJS*, 74, 1075
- Moon, T. 1985, *Ap&SS*, 117, 261
- Moon, T. T. & Dworetsky, M. M. 1985, *MNRAS*, 217, 305
- Napiwotzki, R., Schönberner, D., & Wenske, V. 1993, *A&A*, 268, 653
- Neuforge-Verheecke, C. & Magain, P. 1997, *A&A*, 328, 261
- Popper, D. M. 1980, *ARA&A*, 18, 115
- . 1993, *ApJ*, 404, L67
- Pottasch, E. M., Butcher, H. R., & van Hoesel, F. H. J. 1992, *A&A*, 264, 138
- Pourbaix, D., Neuforge-Verheecke, C., & Noels, A. 1999, *A&A*, 344, 172
- Qiu, H., Zhao, G., Chen, Y. Q., & Li, Z. W. 2001, *A&A*, 548, 953
- Relyea, L. J. & Kurucz, R. L. 1978, *ApJS*, 37, 45
- Rentzsch-Holm, I. 1997, *A&A*, 317, 178
- Russell, S. C. & Bessell, M. S. 1989, *ApJS*, 70, 865
- Sadakane, K. & Nishimura, M. 1981, *PASJ*, 33, 189
- Sadakane, K. & Ueta, M. 1989, *PASJ*, 41, 279
- Smalley, B. & Dworetsky, M. M. 1993, *A&A*, 271, 515
- . 1995, *A&A*, 293, 446
- Smalley, B. & Kupka, F. 1997, *A&A*, 328, 349
- Smith, G., Edvardsson, B., & Frisk, U. 1986, *A&A*, 165, 126
- Smith, K. C. & Dworetsky, M. M. 1993, *A&A*, 274, 335
- Smith, V. V. & Lambert, D. L. 1986, *ApJ*, 311, 843
- Soderblom, D. R. 1986, *A&A*, 158, 273
- Sokolov, N. A. 1995, *A&AS*, 110, 553
- Spite, F., Spite, M., & Francois, P. 1989, *A&A*, 210, 25
- Venn, K. A. & Lambert, D. L. 1990, *ApJ*, 363, 234
- Volk, K. & Cohen, M. 1989, *AJ*, 98, 1918

ISO-SWS calibration and the accurate modelling of cool-star atmospheres ^{*}

III. A0 to G2 stars

L. Decin^{1**}, B. Vandenbussche¹, C. Waelkens¹, K. Eriksson², B. Gustafsson², B. Plez³, and A.J. Sauval⁴

¹ Instituut voor Sterrenkunde, KULeuven, Celestijnenlaan 200B, B-3001 Leuven, Belgium

² Institute for Astronomy and Space Physics, Box 515, S-75120 Uppsala, Sweden

³ GRAAL - CC72, Université de Montpellier II, F-34095 Montpellier Cedex 5, France

⁴ Observatoire Royal de Belgique, Avenue Circulaire 3, B-1180 Bruxelles, Belgium

Received data; accepted date

Abstract. Vega, Sirius, β Leo, α Car and α Cen A belong to a sample of twenty stellar sources used for the calibration of the detectors of the Short-Wavelength Spectrometer on board the Infrared Space Observatory (ISO-SWS). While general problems with the calibration and with the theoretical modelling of these stars are reported in Decin et al. (2002), each of these stars is discussed individually in this paper. As demonstrated in Decin et al. (2002), it is not possible to deduce the effective temperature, the gravity and the chemical composition from the ISO-SWS spectra of these stars. But since ISO-SWS is absolutely calibrated, the angular diameter (θ_d) of these stellar sources can be deduced from their ISO-SWS spectra, which consequently yields the stellar radius (R), the gravity-inferred mass (M_g) and the luminosity (L) for these stars. For Vega, we obtained $\theta_d = 3.35 \pm 0.20$ mas, $R = 2.79 \pm 0.17 R_\odot$, $M_g = 2.54 \pm 1.21 M_\odot$ and $L = 61 \pm 9 L_\odot$; for Sirius $\theta_d = 6.17 \pm 0.38$ mas, $R = 1.75 \pm 0.11 R_\odot$, $M_g = 2.22 \pm 1.06 M_\odot$ and $L = 29 \pm 6 L_\odot$; for β Leo $\theta_d = 1.47 \pm 0.09$ mas, $R = 1.75 \pm 0.11 R_\odot$, $M_g = 1.78 \pm 0.46 M_\odot$ and $L = 15 \pm 2 L_\odot$; for α Car $\theta_d = 7.22 \pm 0.42$ mas, $R = 74.39 \pm 5.76 R_\odot$, $M_g = 12.80^{+24.95}_{-6.35} M_\odot$ and $L = 14573 \pm 2268 L_\odot$ and for α Cen A $\theta_d = 8.80 \pm 0.51$ mas, $R = 1.27 \pm 0.08 R_\odot$, $M_g = 1.35 \pm 0.22 M_\odot$ and $L = 1.7 \pm 0.2 L_\odot$. These deduced parameters are confronted with other published values and the goodness-of-fit between observed ISO-SWS data and the corresponding synthetic spectrum is discussed.

Key words. Infrared: stars – Stars: atmospheres – Stars: fundamental parameters – Stars: individual: Vega, Sirius, Denebola, Canopus, α Cen A

1. Introduction

In the first two papers of this series (Decin et al. 2000, 2002, hereafter referred to as Paper I and Paper II respectively), a method is described to analyze a sample of ISO-SWS spectra of standard stars in a consistent way. We did not only concentrate on the possibility to extract reliable stellar parameters from the medium-resolution ISO-SWS spectra, but have also demonstrated where problems in the computation of synthetic spectra — based on the MARCS and Turbospectrum code (Gustafsson et al. 1975; Plez et al. 1992, 1993), version May 1998 — and in the cal-

ibration of the ISO-SWS detectors destroy the goodness-of-fit between observed and synthetic spectra (Paper II). These general results were based on a sample of 5 warm ($T_{\text{eff}} > T_{\text{eff},\odot}$) and 11 cool stars. In this paper, we will further analyse these 5 warm stars — α Cen A, β Leo, α Car, Sirius and Vega — in order to extract relevant astrophysical data.

After a description of the general problems for these warm stars in Sect. 2 (as described in Paper II), we will outline the method of analysis to deduce different stellar parameters in Sect. 3 (based on the results of Paper I and Paper II). In the different subsections of Sect. 3, each star will be discussed individually. In order to assess the observed accuracy, some specific calibration details will be given. If available, different AOT01 observations¹ (i.e. a full SWS scan at reduced spectral resolution, with four

Send offprint requests to: L. Decin, e-mail: Leen.Decin@ster.kuleuven.ac.be

^{*} Based on observations with ISO, an ESA project with instruments funded by ESA Member States (especially the PI countries France, Germany, the Netherlands and the United Kingdom) and with the participation of ISAS and NASA.

^{**} Postdoctoral Fellow of the Fund for Scientific Research, Flanders

¹ Each observation is determined uniquely by its observation number (8 digits), in which the first three digits represent the revolution number. The observing data can be calculated from

possible scan speeds) are compared with each other to demonstrate the calibration precision of ISO-SWS. With these remarks in mind, the synthetic spectrum based on assumed and deduced parameters is confronted with the ISO-SWS spectrum. Furthermore, we will discuss why we have assumed certain parameters and we will confront the deduced parameters from the ISO-SWS spectra with other literature values.

The appendix of this article is published electronically. Most of the grey-scale plots in the article are printed in colour in the appendix, in order to better distinguish the different spectra.

2. Summary of general discrepancies (Paper II)

For the warm stars in our sample, the origin of the general discrepancies between the ISO-SWS and synthetic spectra could be reduced to 1. inaccurate atomic oscillator strengths in the infrared, 2. problematic computation of hydrogenic line broadening, 3. fringes at the end of band 1D (3.02 – 3.52 μm), 4. inaccurate Relative Spectral Response Function (RSRF) at the beginning of band 1A (2.38 – 2.60 μm) and 5. memory effects in band 2 (4.08 – 12.00 μm).

3. Stellar parameters

In Paper I of this series, a method was described to determine stellar parameters from the band-1 data (2.38 – 4.08 μm) of ISO-SWS spectra. This method was based on the presence of different molecular absorbers in this wavelength range, each having their own characteristic absorption pattern. Since the infrared absorption pattern of these A0 – G2 stars is completely dominated by atoms (with the exception of α Cen A, for which the CO first overtone and fundamental bands are weakly visible) this method of analysis could not be applied to these stars. Moreover, it was demonstrated in Paper II that there are still quite some problems with the oscillator strengths of infrared atomic transitions. It was therefore impossible to determine the effective temperature (T_{eff}), the gravity ($\log g$), the microturbulence (ξ_t), the metallicity ($[\text{Fe}/\text{H}]$) and the abundance of carbon, nitrogen and oxygen for these warm stars from their ISO-SWS spectra. In order to further analyze these spectra, we have performed a detailed literature study to find accurate values for these stellar parameters. Using these parameter values, synthetic spectra were computed for each target. From the absolutely calibrated ISO-SWS spectra, we then could deduce the angular diameter (θ_d). The angular diameter together with the Hipparcos' parallax (with the only exception of α Cen A for which a more precise parallax by Pourbaix et al. (1999) is available) then yielded the stellar radius. Together with the assumed gravity and effective temperature, the gravity-inferred mass (M_g) and the stellar luminosity (L) are derived.

the revolution number which is the number of days after 17 November 1995.

The resultant stellar parameters are summarised in Table 1. The objects have been sorted by spectral type. Since the error bars of certain assumed stellar parameters were necessary for the propagation to the mean error of other deduced parameters (see Eq. (18) in Paper I), the error bars on all stellar parameters are given. The mean error on the angular diameter is estimated from the intrinsic error, the absolute flux error (10%) and the error in the assumed effective temperature (see Paper II). Whenever $\sigma(\log g) \geq 0.40$, the lower and upper limit of the gravity-inferred mass M_g are estimated as being 2/3 of the *maximum* error. In the subsequent subsections, each star will be discussed individually. A short description of the methods and/or data used and on the parameters assumed and deduced by the different authors quoted in next sections, can be retrieved from <http://www.ster.kuleuven.ac.be/~leen/artikels/ISO3/appendix.ps>.

3.1. α Cen A: AOT01, speed 4, revolution 607

3.1.1. Some specific calibration details

Since α Cen A is component of a binary, one has to check the flux contribution of the second component (HIC 71681, K1 V). From the coordinates of the system in 1997, its proper motion and the correction for the orbit, one obtains

$$\begin{cases} \alpha_A &= 14\text{h } 39\text{m } 24.13\text{s} \\ \delta_A &= -60\text{deg } 49' 17.9'' \\ \alpha_B &= 14\text{h } 39\text{m } 22.73\text{s} \\ \delta_B &= -60\text{deg } 49' 30.4'' \end{cases}$$

This results in a difference in spacecraft coordinates of $dy = -12.1241''$ and $dz = 10.9342''$. Taking the pointing jitter into account ($\leq 1.5''$), and the fact that the average difference between the G and K star in the wavelength range from 1.6 μm to 11.2 μm is 0.91^m (Cohen et al. 1996a), one can calculate that the maximal flux contribution from the K dwarf around 3 μm is 6 Jy, which is negligible.

The factors, by which the data of the different subbands are multiplied (see Table 3 in Paper II) show a good agreement with the band-border ratios determined by Feuchtgruber (1998). The only exception is band 2C, but this is not so significant, due to the large scatter for the band-border ratio between band 2B and band 2C (Fig. 6 in Feuchtgruber 1998) and the memory effects in band 2.

3.1.2. Comparison with other AOT01 observations

Alpha Cen A has also been observed during revolution 294 with the AOT01 speed-1 option. The pointing offsets were $dy = -0.797''$ and $dz = -0.832''$. Also for this observation, the contribution of the K main-sequence companion of α Cen A is negligible. The data of both band 1B and band 1E have been multiplied by a factor 1.01. The relative features match quite well taking the uncertainties of the speed-1 observation into account. There is, however, a difference in absolute flux level of 16% (Fig. 1). In revolution 294, the

Table 1. Fundamental stellar parameters for the selected stars in the sample. The effective temperature T_{eff} is given in K, the logarithm of the gravity in c.g.s. units, the microturbulent velocity ξ_t in km s^{-1} , the angular diameter in mas, the parallax π in mas, the distance D in parsec, the radius R in R_{\odot} , the gravity-inferred mass M_g in M_{\odot} and the luminosity L in L_{\odot} .

	α Lyr	α CMa	β Leo	α Car	α Cen A
Sp. Type	A0 V	A1 V	A3 Vv	F0 II	G2 V
T_{eff}	9650 ± 200	10150 ± 400	8630 ± 200	7350 ± 300	5830 ± 30
$\log g$	3.95 ± 0.20	4.30 ± 0.20	4.20 ± 0.10	1.80 ± 0.50	4.35 ± 0.05
ξ_t	2.0 ± 0.5	2.0 ± 0.5	2.0	3.25 ± 0.25	1.0 ± 0.1
[Fe/H]	-0.40 ± 0.30	0.50 ± 0.30	0.20	-0.24 ± 0.04	0.25 ± 0.02
$\varepsilon(\text{C})$	8.42 ± 0.15	7.97 ± 0.15	8.76	8.41 ± 0.10	8.74 ± 0.05
$\varepsilon(\text{N})$	8.00 ± 0.15	8.15 ± 0.15	8.25	8.68 ± 0.05	8.26 ± 0.09
$\varepsilon(\text{O})$	8.74 ± 0.15	8.55 ± 0.12	9.13	8.91 ± 0.10	9.13 ± 0.06
θ_d	3.35 ± 0.20	6.17 ± 0.38	1.47 ± 0.09	7.22 ± 0.42	8.80 ± 0.51
π	128.93 ± 0.55	379.21 ± 1.58	90.16 ± 0.89	10.43 ± 0.53	737.0 ± 2.6
D	7.76 ± 0.03	2.63 ± 0.01	11.09 ± 0.11	95.88 ± 4.87	1.36 ± 0.01
R	2.79 ± 0.17	1.75 ± 0.11	1.75 ± 0.11	74.39 ± 5.76	1.27 ± 0.08
M_g	2.54 ± 1.21	2.22 ± 1.06	1.78 ± 0.46	$12.77^{+24.95}_{-6.35}$	1.35 ± 0.22
L	61 ± 9	29 ± 6	15 ± 2	14573 ± 2268	1.7 ± 0.2

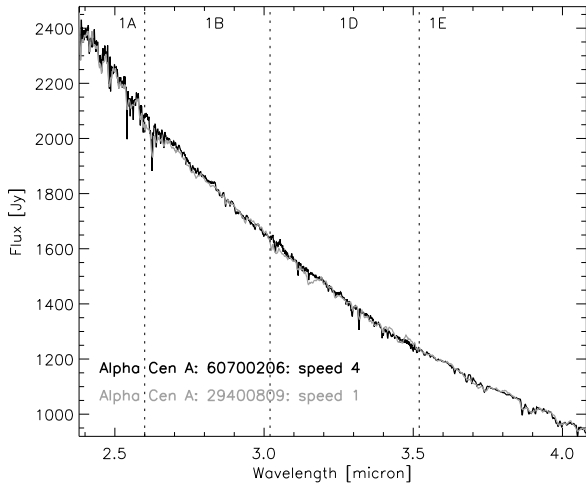


Fig. 1. Comparison between the AOT01 speed-4 observation of α Cen A (revolution 607) and the speed-1 observation (revolution 294). The data of the speed-1 observation have been multiplied by a factor 1.16. A coloured version of this plot is available in the Appendix as Fig. ??.

activation of the scientific measurements was started later than usual because of the time allocated for the Delta-V manoeuvre and the measurement of the superfluid He mass. These two activities may have influenced the quality of the speed-1 observation. As will be argued in a subsequent article in this series — where we will confront the obtained synthetic spectra with the templates of Cohen (Cohen et al. 1992b, 1995, 1996b; Witteborn et al. 1999) — it is reasonable to assume that the absolute flux level of the speed-4 observation is somewhat too high. Since the absolute flux accuracy is quoted to be $\sim 10\%$, this 16% flux-difference is still within the quoted error bar.

3.1.3. Comparison between the ISO-SWS spectrum and the synthetic spectrum (Fig. 2)

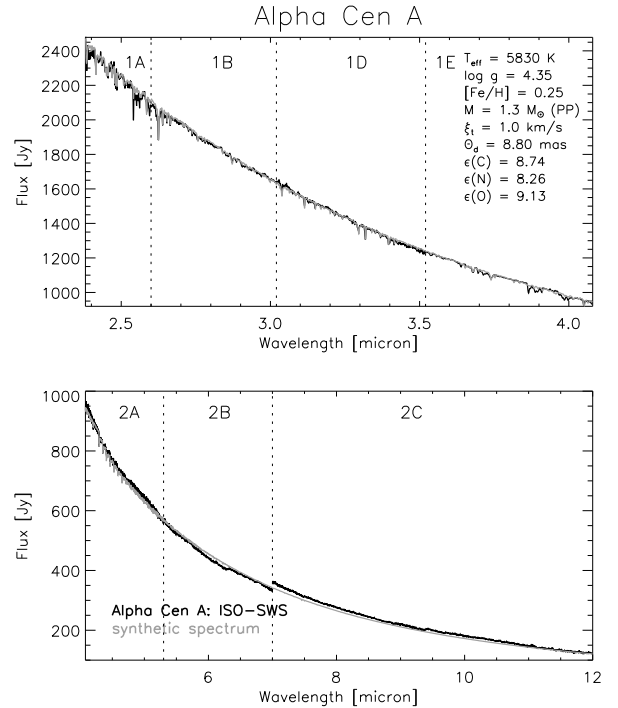


Fig. 2. Comparison between band 1 and band 2 of the ISO-SWS data of α Cen A (black) and the synthetic spectrum (grey) with stellar parameters $T_{\text{eff}} = 5830$ K, $\log g = 4.35$, $M = 1.3 M_{\odot}$, $[\text{Fe}/\text{H}] = 0.25$, $\xi_t = 1.0 \text{ km s}^{-1}$, $\varepsilon(\text{C}) = 8.74$, $\varepsilon(\text{N}) = 8.26$, $\varepsilon(\text{O}) = 9.13$ and $\theta_d = 8.80$ mas. A coloured version of this plot is available in the Appendix as Fig. ??.

As discussed in Paper II, it is quite difficult to pin down the fundamental parameters of α Cen A from the SWS-spectrum, due to the absence of molecular features. Therefore, the parameters found by Neuforge-Verheucke & Magain (1997) were used to calculate the corresponding synthetic spectrum. Subsequently, the angular diameter, radius, mass and luminosity were derived. This resulted in the following parameters: $T_{\text{eff}} = 5830 \pm 30$ K, $\log g = 4.35 \pm 0.05$, $\xi_t = 1.0 \pm 0.1$ km s $^{-1}$, $[\text{Fe}/\text{H}] = 0.25 \pm 0.02$, $\varepsilon(\text{C}) = 8.74 \pm 0.05$, $\varepsilon(\text{N}) = 8.26 \pm 0.09$, $\varepsilon(\text{O}) = 9.13 \pm 0.06$, $\pi = 737.0 \pm 2.6$ mas, $\theta_d = 8.80 \pm 0.51$ mas, $R = 1.27 \pm 0.08 R_{\odot}$, $M_g = 1.35 \pm 0.22 M_{\odot}$ and $L = 1.7 \pm 0.2 L_{\odot}$, with deviation estimating parameters from the Kolmogorov-Smirnov test (see Paper I) being $\beta_{1A} = 0.043$, $\beta_{1B} = 0.036$, $\beta_{1D} = 0.063$, $\beta_{1E} = 0.024$.

Looking to the relative contribution of the different chemical species (see Fig. 3.1 in Decin 2000) and to the Atmospheric Trace Molecule Spectroscopy (ATMOS) spectrum of the Sun (Geller 1992; Gunson et al. 1996), it is obvious that the atoms dominate the infrared spectrum of α Cen A, although the CO fundamental and first-overtone bands start arising around $4.4 \mu\text{m}$ and $2.4 \mu\text{m}$ respectively. As described in Paper II, problems with inaccurate oscillator strengths of the atomic lines in the infrared in the line list of Hirata & Horaguchi (1995) caused quite some discrepancies between the ISO-SWS and synthetic spectra. By using the identifications given by Geller (1992) for the ATMOS solar spectrum, the strongest contributors to the most prominent features were identified, with the strongest lines originating from Fe, Al, Si and Mg transitions (see, e.g., Fig. 5 in Paper II). The largest difference between the ISO-SWS spectrum of α Cen A and the rebinned ATMOS spectrum of the Sun occurs around $2.4 \mu\text{m}$. As discussed in Paper II, the origin of this problem is situated in the problematic RSRF of band 1A in this wavelength region. The problems with the computation of the Humphreys lines near the Humphreys ionisation edge result in β_{1D} being higher than the maximum acceptable value for this sub-band as given in Table 3 in Paper I.

3.1.4. Comparison with other published stellar parameters

– Assumed parameters:

It has to be noted that the fundamental stellar parameters (T_{eff} , $\log g$, ξ_t , $[\text{Fe}/\text{H}]$, $\varepsilon(\text{C})$, $\varepsilon(\text{N})$, $\varepsilon(\text{O})$), determined by several authors using different methods, are in excellent agreement (see Table 2). Since the most up-to-date spectroscopic analysis based on high-resolution and high signal-to-noise spectra of α Cen A was performed by Neuforge-Verheucke & Magain (1997), their derived parameters were used as input parameters.

– Deduced parameters:

The angular diameter deduced from the AOT01 speed-4 observation of α Cen A (revolution 607), is somewhat larger than the values obtained by other indirect methods, but is still within the error bars of the

other values. The origin of the difference may be too high a flux level of the ISO-SWS AOT01 speed-4 observation (see Sect. 3.1.2). As a consequence, the stellar radius, gravity-inferred mass and luminosity are also somewhat larger than the other values listed in Table 2. Different methods were used by different authors to estimate the radius of α Cen A: using T_{eff} and L (e.g., Soderblom 1986; Furenlid & Meylan 1990), using θ_d and π (e.g., Volk & Cohen 1989) or using the p-mode oscillations found in α Cen A (e.g., Pottasch et al. 1992). The same can be said for the luminosity, where Flannery & Ayres (1978) have used different broad-band systems and narrow-band photometric indices to estimate the luminosity; Volk & Cohen (1989) and Pottasch et al. (1992) have used the assumed T_{eff} and deduced R-values. The most quoted mass value for α Cen A is the one deduced by Demarque et al. (1986) ($M = 1.085 \pm 0.010 M_{\odot}$). Pourbaix et al. (1999) found for the first time an agreement between astrometric and spectroscopic mass ratio. Their value for the mass ($M = 1.160 \pm 0.031 M_{\odot}$) is in better agreement with a mass estimated from the evolutionary tracks of Girardi et al. (2000) (for $T_{\text{eff}} = 5830$ K and $L = 1.7 L_{\odot}$, we found $M = 1.02 \pm 0.20 M_{\odot}$) than our gravity-inferred mass of $1.30 \pm 0.21 M_{\odot}$.

3.2. α Car : AOT01, speed 4, revolution 729

3.2.1. Some specific calibration details

Only the band-1A flux had to be multiplied with a factor larger than 1.02, although this is still smaller than the mean band-border ratio between band 1A and band 1B for that revolution (see Fig. 1 in Feuchtgruber, 1998).

3.2.2. Comparison between the ISO-SWS spectrum and the synthetic spectrum (Fig. 3)

Using the stellar parameters $T_{\text{eff}} = 7350$ K, $\log g = 1.80$, $\xi_t = 3.25$ km s $^{-1}$, $[\text{Fe}/\text{H}] = -0.24$, $\varepsilon(\text{C}) = 8.41$, $\varepsilon(\text{N}) = 8.68$, $\varepsilon(\text{O}) = 8.91$ (Desikachary & Hearnshaw 1982) and $\pi = 10.43 \pm 0.53$ mas results in $\theta_d = 7.22 \pm 0.42$ mas, $R = 74.39 \pm 5.76 R_{\odot}$, $M_g = 12.80^{+24.95}_{-6.35} M_{\odot}$ and $L = 14573 \pm 2268 L_{\odot}$ with deviation estimating parameters $\beta_{1A} = 0.091$, $\beta_{1B} = 0.045$, $\beta_{1D} = 0.091$, $\beta_{1E} = 0.041$.

Just as for α Cen A, the large β -values from the Kolmogorov-Smirnov test may be explained by the problematic prediction of the atomic lines and especially the hydrogen lines (which dominate the spectral signature) and the noise. The more pronounced discrepancy visible at the beginning of band 1A is due to calibration problems (RSRF). The lower gravity of α Car with respect to the other *warm* stars is reflected in the smaller broadening of the hydrogen lines. Despite this lower gravity, all but one sub-band are rejected by the Kolmogorov-Smirnov test.

Table 2. Literature study of α Cen A, with the effective temperature T_{eff} given in K, the mass M in M_{\odot} , the microturbulent velocity ξ_t in km/s, the angular diameter θ_d in mas, the luminosity L in L_{\odot} and the radius R in R_{\odot} . Angular diameters deduced from direct measurements (e.g from interferometry) are written in italic, while others (e.g. from spectrophotometric comparisons) are written upright. Assumed or adopted values are given between parentheses. The results of this research are mentioned in the last line. Only the error bars on the *deduced* parameters are given. A short description of the methods and/or data used by the several authors can be retrieved from <http://www.ster.kuleuven.ac.be/~leen/artikels/ISO3/appendix.ps>.

T_{eff}	log g	M	ξ_t	[Fe/H]	$\varepsilon(\text{C})$	$\varepsilon(\text{N})$	$\varepsilon(\text{O})$	θ_d	L	R	Ref.
5800								8.62 ± 0.23			1.
5800 ± 100		1.11 ± 0.03							1.51 ± 0.06		2.
		1.10									3.
5750 ± 30	4.38 ± 0.07	1.08	1.0	0.28 ± 0.15							4.
		1.085 ± 0.010									5.
5820 ± 50	4.40 ± 0.05		1.54 ± 0.08	0.20 ± 0.04							6.
5770 ± 20										1.23	7.
(5770)	4.5		(1.0)	0.22 ± 0.15							8.
(5750)	4.42 ± 0.11		(1.5)	(0.28)							9.
5700 ± 75									1.446	1.23 ± 0.03	10.
5710 ± 25	4.27 ± 0.20	(1.085)	1.0 ± 0.2	0.12 ± 0.06	8.77 ± 0.04		8.98 ± 0.06			1.26	11.
5834 ± 140											12.
5800 ± 20	4.31 ± 0.02	(1.085)	(1.0)	0.22 ± 0.02							13.
5760								8.52			14.
5710		(1.085)							1.33 ± 0.11	1.17 ± 0.05	15.
	4.3	1.4									16.
(5770)	(4.29)		1.28 ± 0.05 1.17 ± 0.06	0.00							17 ^a .
(5770)	(4.29)		1.48-1.06	0.30							17 ^b .
5830 ± 30	4.34 ± 0.05	(1.085)	1.09 ± 0.11	0.25 ± 0.02	8.74 ± 0.05	8.26 ± 0.09	9.13 ± 0.06		1.5		18.
		1.160 ± 0.031									19.
(5830)	(4.35)	1.35 ± 0.22	(1.0)	(0.25)	(8.74)	(8.26)	(9.13)	8.80 ± 0.51	1.7 ± 0.2	1.27 ± 0.08	20.

1. Blackwell & Shallis (1977); 2. Flannery & Ayres (1978); 3. Kamper & Wesselink (1978); 4. England (1980); 5. Demarque et al. (1986); 6. Smith & Lambert (1986); 7. Soderblom (1986); 8. Abia et al. (1988); 9. Edvardsson (1988); 10. Volk & Cohen (1989); 11. Furenlid & Meylan (1990); 12. McWilliam (1990); 13. Chmielewski et al. (1992); 14. Engelke (1992); 15. Pottasch et al. (1992); 16. Popper (1993); 17. Gadun (1994); 18. Neuforge-Verheecke & Magain (1997); 19. Pourbaix et al. (1999); 20. present results

Table 3. See caption of Table 2, but now for α Car.

T_{eff}	log g	M	ξ_t	[Fe/H]	$\varepsilon(\text{C})$	$\varepsilon(\text{N})$	$\varepsilon(\text{O})$	θ_d	L	R	Ref.
7460 ± 460								6.6 ± 0.8			1.
7206 ± 173								(6.6)			2.
7420								7.08 ± 0.19			3.
7500 ± 200	1.85 ± 0.30		2.7 ± 1.0	0.35 ± 0.15							4.
7346 ± 150								6.81 ± 0.20			5.
7350 ± 300	1.80 ± 0.50		3.25 ± 0.25	-0.24 ± 0.04	8.41 ± 0.10	8.68 ± 0.05	8.91 ± 0.10				6.
7400 ± 150	1.9 ± 0.2		4.5 6.0								7.
(7400)	(1.9)	8 ± 1.5	(4.5)	-0.10	8.32				7500	53	8.
7320 - 7900	1.8 ± 0.2		3.0								10 ^a .
7500 ± 200	1.5 ± 0.3		3.5 ± 0.5	-0.07	8.27	8.24	8.69				10 ^b .
								6.6 ± 0.8			11.
7260 ± 200	1.83 ± 0.30										12 ^a .
(7400)	(1.9)	7.94	4.5 5.7	-0.12	7.33					52.48	12 ^b .
(7500)	1.2		3.0	+0.08 ± 0.10							13.
7460 ± 460									(1795)	25.5 ± 3.9	14.
7298 ± 150											15.
7500 ± 100	1.2 ± 0.2	8-9	2.8 ± 0.2	0.00							16.
(7500)	(1.5)	12.6									17.
7350	1.80	8	1.99-4.27 2.40-5.44	-0.3 ± 0.11						53	18.
7500 ± 200	1.5 ± 0.3		2.5 ± 0.5	0.06 ± 0.15	8.41 ± 0.10		8.63 ± 0.2				19.
7520 ± 460	< 1.5							(6.6)			20.
(7350)	(1.80)	12.8 ^{+24.95} _{-6.35}	(3.25)	(-0.25)	(8.41)	(8.68)	(8.91)	7.22 ± 0.42	14573 ± 2268	74.39 ± 5.76	21.

1. Brown et al. (1974); 2. Code et al. (1976); 3. Blackwell & Shallis (1977); 4. Linsky & Ayres (1978); 5. Luck (1979); 6. Blackwell et al. (1980); 7. Desikachary & Hearnshaw (1982); 8. Boyarchuk & Lyubimkov (1983); 9. Lyubimkov & Boyarchuk (1984); 10. Luck & Lambert (1985); 11. di Benedetto & Rabbia (1987); 12. Russell & Bessell (1989); 13. Spite et al. (1989); 14. Volk & Cohen (1989); 15. McWilliam (1990); 16. Achmad et al. (1991); 17. El Eid (1994); 18. Gadun (1994); 19. Hill et al. (1995); 20. Smalley & Dworetzky (1995); 21. present results

3.2.3. Comparison with other published stellar parameters

– Assumed parameters:

From Table 3, it is clearly apparent that a gravity deter-

mined in a spectroscopic way (i.e. by requiring that the abundance of neutral and ionised lines yield the same abundance) is usually lower than a photometric gravity (i.e. determined from photometric colours, or by

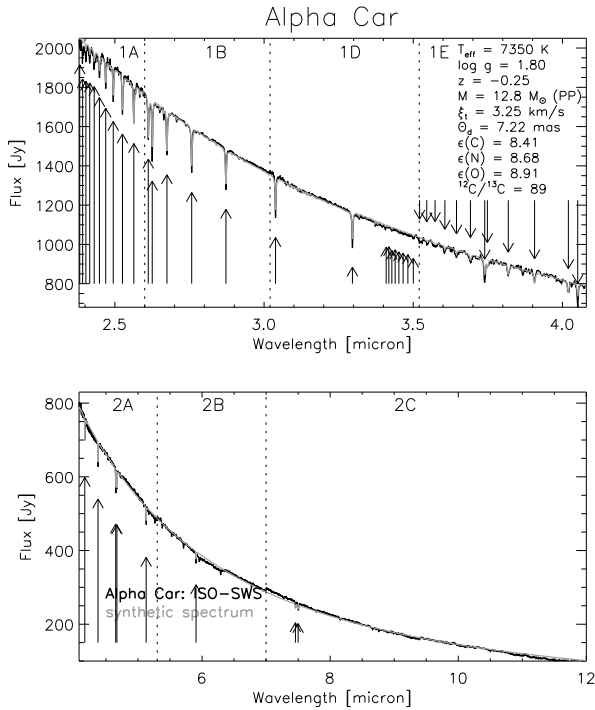


Fig. 3. Comparison between band 1 and band 2 of the ISO-SWS data of α Car (black) and the synthetic spectrum (grey) with stellar parameters $T_{\text{eff}} = 7350$ K, $\log g = 1.80$, $M = 12.8 M_{\odot}$, $[\text{Fe}/\text{H}] = -0.25$, $\xi_t = 3.25$ km s $^{-1}$, $\epsilon(\text{C}) = 8.41$, $\epsilon(\text{N}) = 8.68$, $\epsilon(\text{O}) = 8.91$ and $\theta_d = 7.22$ mas. Hydrogen lines are indicated by arrows. A coloured version of this plot is available in the Appendix as Fig. ??.

using the well-known relation between g , T_{eff} , M and L , where the mass has been determined by locating the stellar object on theoretical evolutionary tracks). It is well known that the accuracy of spectroscopic determinations of gravities from ionisation equilibria or molecular equilibria for individual stars is not very good for giants (cf., e.g., Trimble & Bell 1981; Brown et al. 1983; Smith & Lambert 1985). Therefore, the values given by Desikachary & Hearnshaw (1982) were adopted as atmospheric parameters for α Car.

– Deduced parameters:

The angular diameter derived from the ISO-SWS data is larger than the two values based on the InfraRed Flux Method (IRFM, Blackwell & Shallis 1977; Blackwell et al. 1980) in Table 3. Napiwotzki et al. (1993) quoted that temperatures deduced by using the IRFM are *too low* by 1.6 – 2.8%, corresponding to angular diameters which are too large by 3.5 – 5.9%. When inspecting the other stars of the sample which have been analysed by means of the IRFM, this trend however is not visible. The reason for the discrepancy in angular diameter may be the problematic determination of the continuum in the spectrum of a *warm* star (Paper II). This larger angular diameter however can not explain the difference in radius and luminos-

ity seen between our results and other literature values. Lyubimkov & Boyarchuk (1984) have estimated a mass value of $8 \pm 1.5 M_{\odot}$ for α Car from the evolutionary tracks of Becker (1981) in the $\log T_{\text{eff}} - \log g$ plane. Also Russell & Bessell (1989) have determined the mass from evolutionary tracks. Together with the gravity mentioned by Boyarchuk & Lyubimkov (1983), this results in the stellar radius of $\sim 53 R_{\odot}$. Using $V - I = 0.44$ (Johnson et al. 1966), the bolometric correction BC_I from Bessell et al. (1998) and the Hipparcos' parallax, we obtain $M_{\text{bol}} = -5.68 \pm 0.12$ ($L = 14723 \pm 1654 L_{\odot}$), in agreement with our T_{eff} based luminosity. From the evolutionary tracks of Claret & Gimenez (1995) we estimate a somewhat higher mass value being $10.5 \pm 0.5 M_{\odot}$. When our gravity-inferred mass of $12.8 M_{\odot}$ would have been used by Lyubimkov & Boyarchuk (1984) and Russell & Bessell (1989), a stellar radius of $67 R_{\odot}$ and a luminosity of $12000 L_{\odot}$ would have been deduced, in close agreement with our results. Volk & Cohen (1989) found a luminosity of $1795 \pm 71 L_{\odot}$. This value was determined from the effective temperature, which was deduced directly from the literature values of angular diameter measurements, total-flux observations (from the literature) and the parallax from Hoffleit & Jaschek (1982). The parallax value mentioned by Hoffleit & Jaschek (1982) ($\pi = 28$ mas) is however a factor 2.68 higher than the value given by the Hipparcos catalogue. Using the Hipparcos' parallax would increase the stellar radius by the same amount — resulting in $R = 68 R_{\odot}$ — and the luminosity by a factor 7.2 — giving $L \approx 13000 L_{\odot}$, both values now being in good agreement with our deduced values.

3.3. β Leo : AOT01, speed 3, revolution 189

3.3.1. Some specific calibration details

β Leo is one of the few stars of our sample for which no speed-4 observation has been obtained. The signal-to-noise is therefore smaller than for the other *warm* stars. The shape of the spectrum in band 2 (after application of a standard calibration procedure) is very suspicious. A quick-look at the SPD (= Standard Processed Data, which gives the signal as a function of time) reveals immediately the origin of the problem. A photometric check is taken between the measurements with aperture 1 and aperture 2 and between the measurements with aperture 2 and aperture 3, i.e. just before the up scan of band 2A, and before the up scan of band 2C (Fig. 4). The calibration source is, however, much brighter than β Leo, resulting in a strong memory effect. Only the dark current before each measurement (at a certain aperture) has the same reset time as the measurement itself and could be used to subtract the dark current. Since the dark current before the measurement with aperture 3 (band 2C) is strongly affected by memory effects arising from the photometric check, the mean flux value of the dark current is

higher than the flux values of the down scan beyond $9\ \mu\text{m}$. Therefore only the up scan of band 2C is used, and the fact is taken into account that memory effects are destroying the reliability of this up scan. In order to correct for this too high dark current, the data of band 2C are shifted upwards by $3.5\ \text{Jy}$ (Table 3 in Paper II). The other factors used to combine the different sub-bands may also be found in Table 3 in Paper II.

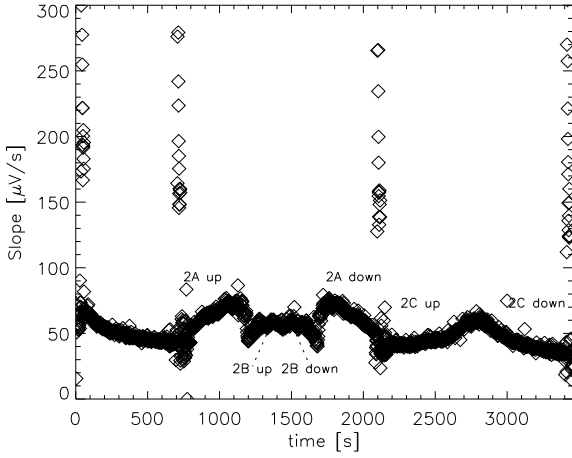


Fig. 4. The slope of detector 13 of band 2 of the AOT01 observation of β Leo (revolution 189) is plotted against time. The up and down scans of the different sub-bands are indicated. Photometric checks are taken between aperture 1 and aperture 2 and between aperture 2 and aperture 3.

3.3.2. Comparison with other AOT01 observations

β Leo has also been observed in revolution 040 during PV (Performance Verification) with the AOT01 speed-1 option. The pointing offsets were $dy = -0.737''$ and $dz = 0.913''$. Due to the triangular shape of the instrumental beam profile in the cross-dispersion direction of SWS, a pointing offset in the cross-dispersion direction causes a higher signal loss than in the dispersion-direction. For this observation, a photometric check was only taken before the up scan of band 2A and after the down scan of band 2C. So, only the up scan of band 2A can be affected by memory effects originating from the photometric check. The down scan of band 2A (and band 1D) displays however a signal jump 640 s after the start of the observation (Fig. 5). The origin of such signal jumps is at the moment unclear (Leech et al. 2002, p. 66). The jumps in bands 1 and 2 are similar to each other, but different from jumps in band 3. They can be negative or positive, and there seems to be a relation between the signal jump and a residual pulse effect after reset. It is recommended to adjust the baseline of the affected portion to the pre-jump baseline. For reason of safety, these data have been flagged as ‘no-

data’. In order to obtain a smooth spectrum, the data of the sub-bands 1A, 1B and 1E of this speed-1 observation have been multiplied by a factor 1.01.

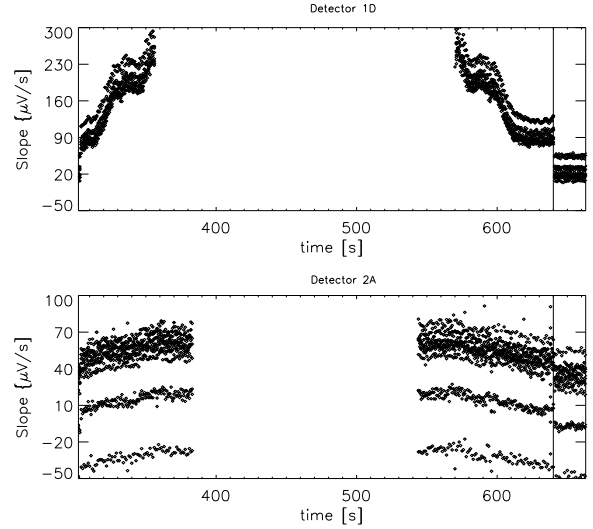


Fig. 5. The slope of the detectors in band 1D and band 2A of the AOT01 speed-1 observation of β Leo (revolution 040) are plotted against time. The signal jump is indicated by the vertical line.

The photometric flux level of this observation (revolution 040) is about 5% lower than the AOT01 speed-4 observation taken during revolution 189. A few differences between the two observed spectra are somewhat more pronounced, e.g. around $2.42\ \mu\text{m}$, $2.58\ \mu\text{m}$, $3.8\ \mu\text{m}$ (see Fig. 6). Inaccuracies in the speed-1 observations — clearly visible from the comparison between up and down scan — originate from these discrepancies.

3.3.3. Comparison between the ISO-SWS spectrum and the synthetic spectrum (Fig. 7)

Good-quality published stellar parameters for β Leo were found in Holweger & Rentzsch-Holm (1995). These authors list as parameters: $T_{\text{eff}} = 8630\ \text{K}$, $\log g = 4.20$. Using Strömgren photometry, Gardiner et al. (1999) obtained $\text{Fe}/\text{H} \approx +0.2$ dex. A microturbulent velocity of $2\ \text{km s}^{-1}$ was assumed. With an angular diameter deduced from the ISO-SWS spectrum $\theta_d = 1.47 \pm 0.09\ \text{mas}$, one obtains $R = 1.75 \pm 0.11 R_{\odot}$, $M_g = 1.78 \pm 1.04 M_{\odot}$ and $L = 15 \pm 3 L_{\odot}$. The corresponding deviation estimating parameters are $\beta_{1A} = 0.060$, $\beta_{1B} = 0.028$, $\beta_{1D} = 0.087$, $\beta_{1E} = 0.038$.

The large β -values for β Leo are not very surprising. One first of all has to take into account the problems with the hydrogen lines, which dominate the spectrum. Secondly, for band 1A, there is also a large discrepancy at the wavelengths where the H5-23 and H5-22 lines emerge at the beginning of this band. A problem with the RSRF is at the origin of this discrepancy (Paper II). The large β_{1D} -value is arising from the problems nearby the Humphreys

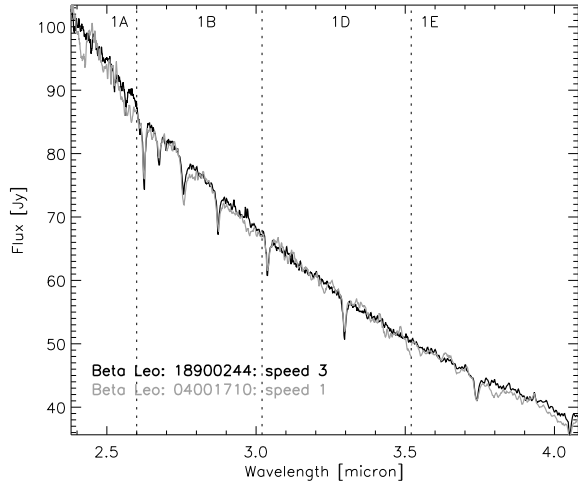


Fig. 6. Comparison between the AOT01 speed-3 observation of β Leo (revolution 189) and the speed-1 observation (revolution 040). The data of the speed-1 observation have been multiplied by a factor 1.05. A coloured version of this plot is available in the Appendix as Fig. ??.

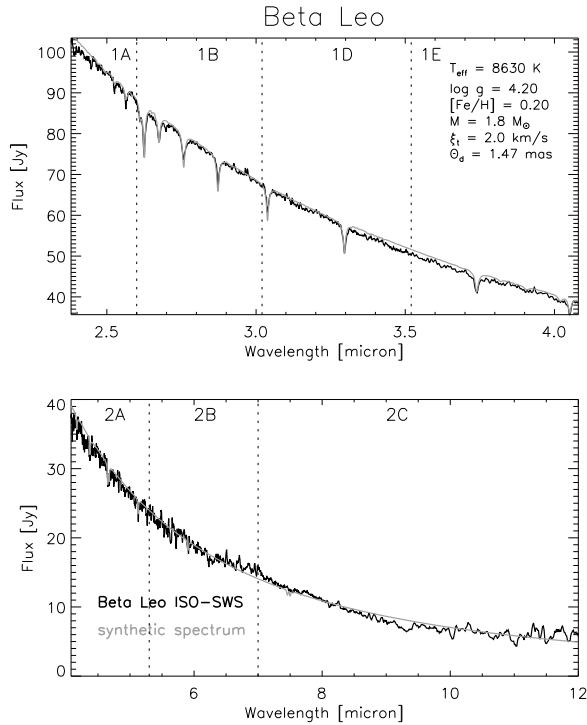


Fig. 7. Comparison between band 1 and band 2 of the ISO-SWS data of β Leo (black) and the synthetic spectrum (grey) with stellar parameters $T_{\text{eff}} = 8630$ K, $\log g = 4.20$, $M = 1.8 M_{\odot}$, $[\text{Fe}/\text{H}] = 0.20$, $\xi_t = 2.0 \text{ km s}^{-1}$ and $\theta_d = 1.47$ mas. A coloured version of this plot is available in the Appendix as Fig. ??.

ionisation edge (Paper II). The lower signal/noise ratio

in a AOT01 speed-3 observation compared to the other observations also contributes to larger β -values.

3.3.4. Comparison with other published stellar parameters

– Assumed parameters:

From the detailed investigation by Smalley & Dworetsky (1993), one may conclude that atmospheric parameters derived from photometry, spectrophotometry and from $\text{H}\beta$ and $\text{H}\gamma$ profiles all agree quite well, provided that adequate opacities and metallicities are used. Especially the values of the effective temperature and gravity should be very reliable when determined from photometry, and they should not be significantly affected by uncertainties in the metallicity (Smalley & Dworetsky 1993). From the research of Gardiner et al. (1999), one may however conclude that the determination of the effective temperature and the gravity for this star from Balmer line profiles (as done e.g. by Smalley & Dworetsky 1995) seems to be rather uncertain, because β Leo is located close to the maximum of the Balmer line width. Therefore, the values found by Holweger & Rentzsch-Holm (1995) — who have used Strömgren photometry — were taken as stellar parameters for the theoretical model and corresponding synthetic spectrum. Since Gardiner et al. (1999) estimated β Leo to be slightly overabundant ($[\text{Fe}/\text{H}] \approx +0.2$ dex) from Strömgren photometry, this value was assumed for the metallicity. For the microturbulent velocity a value of 2 km s^{-1} was assumed.

– Deduced parameters:

Malagnini & Morossi (1990, 1997) have used a flux-fitting method which determines simultaneously the effective temperature and the angular diameter. Their obtained values agree well with the angular diameter deduced from the ISO-SWS spectrum. The small differences in the luminosity and radius values mentioned by Malagnini & Morossi (1990) are partly due to the use of the parallax value of Hoffleit & Jaschek (1982), which is a factor 1.1 lower than the Hipparcos' parallax. When we then compare our gravity-inferred mass with the mass estimated from evolutionary tracks by Malagnini & Morossi (1990), we see that our deduced value is somewhat lower than their quoted value. Using $\log T_{\text{eff}} = 3.936$ and $\log L = 1.176 \pm 0.058$, we estimated from the evolutionary tracks of Girardi et al. (2000) a mass of $1.9 M_{\odot}$, which is thus somewhat closer to the value of $2.3 M_{\odot}$, given by Malagnini & Morossi (1990).

3.4. Sirius: AOT01, speed 4, revolution 689

3.4.1. Some specific calibration details

The speed-4 observation of Sirius only suffered from very small pointing errors. Bands 1A and 1B were shifted upwards by 1 %, band 1E was shifted downwards by 0.5 %.

Table 4. See caption of Table 2, but now for β Leo.

T_{eff}	$\log g$	M	ξ_t	[Fe/H]	$\varepsilon(\text{C})$	$\varepsilon(\text{N})$	$\varepsilon(\text{O})$	θ_d	L	R	Ref.
8850 \pm 340								1.33 \pm 0.10 (1.33) 1.32			1. 2. 3.
8660										1.73	4 ^a .
8660										1.68	4 ^b .
8600	4.2										5.
9590 \pm 460	4.27 \pm 0.15	2.3						1.39 \pm 0.03	25.1 \pm 7.2	1.82 \pm 0.18	6.
8850											7.
8500	4.20			0.00							8 ^a .
8640	4.37			0.50							8 ^b .
8310	4.20			0.00							8 ^c .
8260	4.37			0.50							8 ^d .
8630	4.21										9.
8870 \pm 350	4.00 \pm 0.25							(1.40)			10 ^a .
8870 \pm 350	4.10 \pm 0.30							(1.33)			10 ^b .
8720 \pm 300											11.
8857 \pm 185	4.0							1.374 \pm 0.033			12.
(8870)	(4.10)			0.20							13.
(8630)	(4.20)	1.78 \pm 0.46	(2.0)	(0.00)	(8.76)	(8.25)	(9.13)	1.47 \pm 0.09	15 \pm 2	1.75 \pm 0.11	14.

1. Brown et al. (1974); 2. Code et al. (1976); 3. Moon (1985); 4. Moon & Dworetzky (1985); 5. Lester et al. (1986); 6. Malagnini & Morossi (1990); 7. Napiwotzki et al. (1993); 8. Smalley & Dworetzky (1993); 9. Holweger & Rentzsch-Holm (1995); 10. Smalley & Dworetzky (1995); 11. Sokolov (1995); 12. Malagnini & Morossi (1997); 13. Gardiner et al. (1999); 14. present results

3.4.2. Comparison with other AOT01 observations

At the end of the ISO mission — during revolution 868 — Sirius was once more observed using the AOT01 mode, but now with a higher speed, resulting in a lower resolution and a lower signal-to-noise ratio. The pointing offsets were negligible. Only the data of band 1A were divided by a factor 1.01 to optimize the match between the different sub-bands. The absolute-flux levels differ however by 12 % (Fig. 8). With a quoted absolute-flux accuracy of 10 % and the template of Cohen (Cohen et al. 1992a) being in absolute-flux level in between these two observations this difference is not worrying.

Taking the lower signal-to-noise ratio of the speed-1 observation into account, the features of the two observational spectra of Sirius do agree well.

3.4.3. Comparison between the ISO-SWS spectrum and the synthetic spectrum (Fig. 9)

For Sirius the effective temperature, the gravity and the metallicity were taken from Bell & Dreiling (1981), while the microturbulence and the abundances of C, N and O are the values found by Lambert et al. (1982) who have used the model parameters found by Bell & Dreiling (1981). The adopted stellar parameters for Sirius are thus $T_{\text{eff}} = 10150$ K, $\log g = 4.30$, $\xi_t = 2.0$ km s⁻¹, $[\text{Fe}/\text{H}] = 0.50$, $\varepsilon(\text{C}) = 7.97$, $\varepsilon(\text{N}) = 8.15$, $\varepsilon(\text{O}) = 8.55$, $\pi = 379.21 \pm 1.58$ mas, resulting in $\theta_d = 6.17 \pm 0.38$ mas, $R = 1.75 \pm 0.11 R_{\odot}$, $M_g = 2.22 \pm 1.06 M_{\odot}$ and $L = 29 \pm 6 L_{\odot}$. Using these parameters, the deviation estimating parameters β from the Kolmogorov-Smirnov statistics are $\beta_{1A} = 0.041$, $\beta_{1B} = 0.017$, $\beta_{1D} = 0.098$ and $\beta_{1E} = 0.027$.

Sirius is the star in our sample with the highest gravity. So, it is not surprising that the synthetic spectrum deviates largely from the observed spectrum in band 1D,

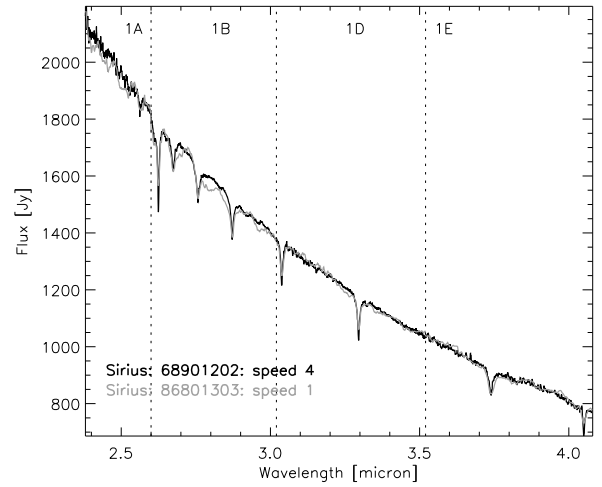


Fig. 8. Comparison between the AOT01 speed-4 observation of α CMA (revolution 689) and the speed-1 observation (revolution 868). The data of the speed-1 observation have been multiplied by a factor 1.12. A coloured version of this plot is available in the Appendix as Fig. ??.

where the Humphreys lines determine the spectral signature. The pronounced discrepancy seen around $6 \mu\text{m}$ is a consequence of the use of an inaccurate model for the memory-effect correction in the OLP6.0 calibration of the ISO-SWS data. Consequently the relative spectral response functions are still not well determined in band 2.

3.4.4. Comparison with other published stellar parameters

– Assumed parameters:

Several authors determined the effective temperature

Table 5. See caption of Table 2, but now for Sirius.

T_{eff}	$\log g$	M	ξ_t	[Fe/H]	$\epsilon(\text{C})$	$\epsilon(\text{N})$	$\epsilon(\text{O})$	θ_d	L	R	Ref.
9697								6.20			1.
(9440)	(4.33)	(2.20)							(23.4)	(1.68)	2.
10150 \pm 400	4.30 \pm 0.20	(2.1)		0.50 \pm 0.30							3.
(10150)	(4.30 \pm 0.20)		2.0 \pm 0.5	0.60 \pm 0.30	7.97 \pm 0.15	8.15 \pm 0.15	8.55 \pm 0.12				4.
								5.89		1.675	5.
9900	4.32										6.
(10000)	(4.30)		2.0	0.50					(26.75)	1.69 \pm 0.05	7.
10100					7.85 \pm 0.06						8.
9900	4.30		2.0		7.82	> 8.20					9.
9870	4.32		1.7 \pm 0.2	0.28							10.
9940 \pm 210	(4.33)	(2.20)									11 ^a .
9940 \pm 210	4.20 \pm 0.15	(2.20)									11 ^b .
9940 \pm 210	4.3 \pm 0.5	(2.20)									11 ^c .
9870 \pm 200	4.40 \pm 0.14		2.0	0.49 \pm 0.29							12.
9900	4.30		2.0	0.64	8.03 \pm 0.54						13.
9945 \pm 122								5.92 \pm 0.09			14 ^a .
9943								5.86			14 ^b .
(9880)	4.40 \pm 0.20		1.85 \pm 0.30	0.50	7.64 \pm 0.06	8.04 \pm 0.15	8.63 \pm 0.05				15.
(10150)	(4.30)	2.22 \pm 1.06	(2.0)	(0.50)	(7.97)	(8.15)	(8.55)	6.17 \pm 0.38	29 \pm 6	1.75 \pm 0.11	16.

1. Blackwell et al. (1980); 2. Popper (1980); 3. Bell & Dreiling (1981); 4. Lambert et al. (1982); 5. Moon (1985); 6. Moon & Dworetzky (1985); 7. Sadakane & Ueta (1989); 8. Volk & Cohen (1989); 9. Lemke (1990); 10. Hill & Landstreet (1993); 11. Smalley & Dworetzky (1995); 12. Hui-Bon-Hoa et al. (1997); 13. Rentzsch-Holm (1997); 14. di Benedetto (1998); 15. Qiu et al. (2001); 16. present results

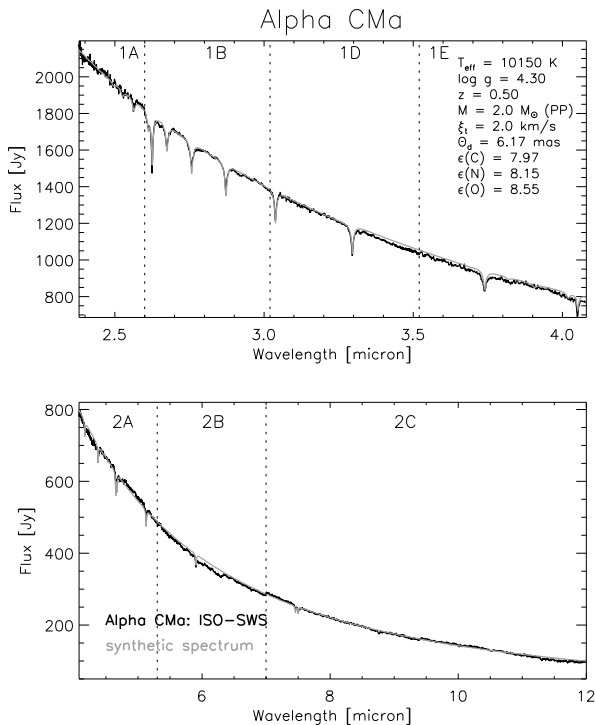


Fig. 9. Comparison between band 1 and band 2 of the ISO-SWS data of α CMa (black) and the synthetic spectrum (grey) with stellar parameters $T_{\text{eff}} = 10150$ K, $\log g = 4.30$, $M = 2.2 M_{\odot}$, $[\text{Fe}/\text{H}] = 0.50$, $\xi_t = 2.0 \text{ km s}^{-1}$, $\epsilon(\text{C}) = 7.97$, $\epsilon(\text{N}) = 8.15$, $\epsilon(\text{O}) = 8.55$ and $\theta_d = 6.17$ mas. A coloured version of this plot is available in the Appendix as Fig. ??.

and the surface gravity for Sirius by using $wby\beta$ photometry and the grids of Moon & Dworetzky (1985) (e.g., Lemke 1990; Hill & Landstreet 1993; Hui-Bon-

Hoia et al. 1997). The values of the effective temperature obtained in that way are in between the values derived from the IRFM (e.g., Blackwell et al. 1980) and the values derived from comparing observed and theoretical fluxes (e.g., Bell & Dreiling 1981), with the IRFM-results being the lowest ones. The derived values for the gravity from the Balmer line profile and from photometric data are in good agreement, and more or less the same abundance pattern is derived by different authors. The microturbulence and C, N and O abundance deduced by Lambert et al. (1982) were assumed as input parameters, who have taken T_{eff} , $\log g$ and $[\text{Fe}/\text{H}]$ from Bell & Dreiling (1981) as model parameters.

– Deduced parameters:

The only indirect measurement of the angular diameter available is from IRFM. Our derived angular diameter of $\theta_d = 6.17 \pm 0.38$ mas corresponds with the value of Blackwell et al. (1980). Contrary to the target α Car, a good agreement is found for the luminosity and radius values of Sirius between our deduced values and the ones of Volk & Cohen (1989). The reason is situated in the Hipparcos' parallax now being almost the same as the parallax of Hoffleit & Jaschek (1982) ($\pi = 378$ mas), used to determine R and L from θ_d . Moon (1985) used a quite different method, based on a new relation between the visual surface brightness F_{ν} and the $(b - y)_0$ colour index of $wby\beta$ photometry (see the appendix available at <http://www.ster.kuleuven.ac.be/~leen/artikels/ISO3/appendix.ps>). His quoted value lies within the error bars of our deduced value.

Not only for Sirius, but also for other warm stars in the sample, we note a large error bar on the derived mass M_g , which mainly depends on the error in the gravity.

This demonstrates that other methods for mass determination (e.g. from data of eclipsing and visual binaries) are far more useful than the underlying method for the M_g determination (from the gravity and the radius).

3.5. Vega: AOT01, speed 3, revolution 178

3.5.1. Some specific calibration details

This speed-3 observation of Vega in revolution 178 had some problems with the pointing: $dy = -0.608''$ and $dz = -1.179''$. Switching then to a larger aperture between band 1B and band 1D results in a flux-jump, which is clearly visible in the factors used to shift the different sub-bands. In order to have a smooth spectrum, we had to multiply the data of bands 1A and 1B by a factor 1.06 (see Table 3 in Paper II).

3.5.2. Comparison between the ISO-SWS spectrum and the synthetic spectrum (Fig. 10)

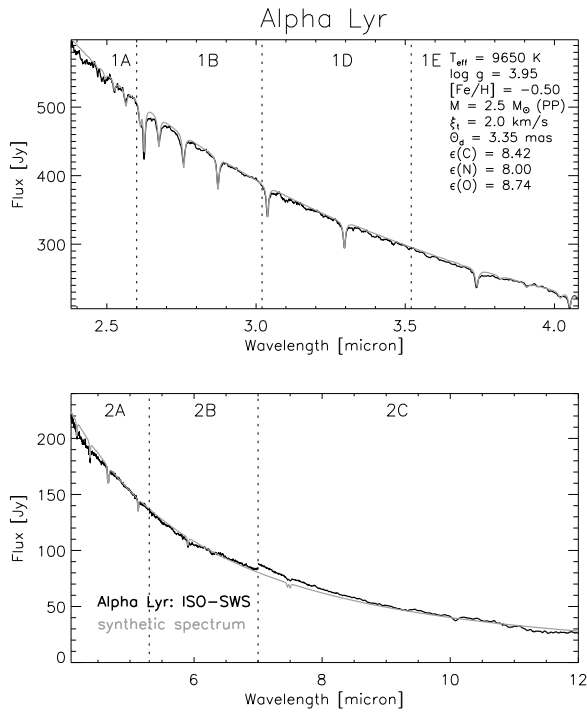


Fig. 10. Comparison between band 1 and band 2 of the ISO-SWS data of α Lyr (black) and the synthetic spectrum (grey) with stellar parameters $T_{\text{eff}} = 9650$ K, $\log g = 3.95$, $M = 2.5 M_{\odot}$, $[\text{Fe}/\text{H}] = -0.50$, $\xi_t = 2.0 \text{ km s}^{-1}$, $\epsilon(\text{C}) = 8.42$, $\epsilon(\text{N}) = 8.00$, $\epsilon(\text{O}) = 8.74$ and $\theta_d = 3.35$ mas. A coloured version of this plot is available in the Appendix as Fig. ??.

As will be discussed in Sect. 3.5.3, the following stellar parameters were adopted for Vega: $T_{\text{eff}} = 9650$ K, $\log g = 3.95$, $\xi_t = 2.0 \text{ km s}^{-1}$, $[\text{Fe}/\text{H}] = -0.50$, $\epsilon(\text{C}) = 8.42$,

$\epsilon(\text{N}) = 8.00$, $\epsilon(\text{O}) = 8.74$. From the ISO-SWS spectrum of Vega, an angular diameter of 3.35 ± 0.20 mas was deduced, which then yields a stellar radius of $2.79 \pm 0.17 R_{\odot}$, a gravity-inferred mass of $2.54 \pm 1.21 M_{\odot}$ and a stellar luminosity of $61 \pm 9 L_{\odot}$. Both the synthetic spectrum based on these parameters and the ISO-SWS spectrum of Vega are displayed in Fig. 10. The corresponding β -values are $\beta_{1A} = 0.057$, $\beta_{1B} = 0.046$, $\beta_{1D} = 0.010$, $\beta_{1E} = 0.041$.

In spite of the lower signal-to-noise and lower resolution of the ISO-SWS observation, good β -values are obtained. One indeed would not expect such a low β -value in band 1D, the wavelength-range in which the hydrogen Humphreys lines are absorbing. The reason for this is twofold: first of all, Vega has the lowest gravity in our sample of main-sequence stars, resulting in a smaller pressure-broadening and thus in smaller hydrogen lines. Consequently, the discrepancy with the synthetic predictions, which underestimate the strength of the Humphreys lines, is not as pronounced as for the other main-sequence stars in our sample. Secondly, Vega has been observed by using the AOT01 speed-3 option and we have already pointed out the small — but visible in the spectrum — mispointing for this observation. The larger noise inherent to this observation can therefore partly camouflage the problem with the theoretical computation of the hydrogen Humphreys lines. Our statistical test will not report this problem, since the Kolmogorov-Smirnov test is a *global* goodness-of-fit test and fitting by eye was still necessary to detect this kind of problems. A new statistical approach in which a *global* and *local* goodness-of-fit test are combined is therefore now under development.

3.5.3. Comparison with other published stellar parameters

The bright star Vega has been studied extensively in recent years because it serves as the primary standard star for photoelectric spectrophotometry. Since so many publications are available for this star — as well as for Sirius — we only have quoted the main publications in the last two decades.

– Assumed parameters:

Inspecting Table 6, we can see that the published values for the different parameters all do agree well. As for Sirius, the temperature values derived from IRFM are somewhat lower than the other published values (see also the remark made by Napiwotzki et al. (1993), who quoted that the IRFM temperatures are too low by 1.6 – 2.8% for main-sequence stars). A detailed study of Vega was made by Dreiling & Bell (1980). From this study Venn & Lambert (1990) have adopted the effective temperature ($T_{\text{eff}} = 9650$ K) and the gravity ($\log g = 3.95$). Using the microturbulent velocity found by Lambert et al. (1982) ($\xi_t = 2.0 \text{ km s}^{-1}$), Venn & Lambert (1990) have determined the chemical composition for Vega. Using the solar metallicity obtained from meteoritic data, $\epsilon(\text{Fe}) = 7.51$, as a reference value,

Table 6. See caption of Table 2, but now for Vega.

T_{eff}	$\log g$	M	ξ_t	[Fe/H]	$\varepsilon(\text{C})$	$\varepsilon(\text{N})$	$\varepsilon(\text{O})$	θ_d	L	R	Ref.
9468								3.35			1.
9650	3.90 ± 0.20	(2.0)		-0.41 ± 0.30				3.24 ± 0.07		2.83	2.
(9660)	(3.94)		2.0	-0.60							3.
(9650)	(3.90)		2.0 ± 0.5	-0.40 ± 0.30	8.57 ± 0.15	7.93 ± 0.15	8.82 ± 0.12				4.
										2.588	5 ^a .
										2.234	5 ^b .
											6.
9500	3.90		2.0	-0.55 ± 0.10							7.
(9500)	(3.90)								(62.66)	2.83 ± 0.13	8.
(9400)	(3.95)		0.6	-0.56 ± 0.15	8.19						9.
9500	3.90				8.49						10.
(9650)	(3.95)		(2.0)	-0.53 ± 0.15	8.42 ± 0.15	8.00 ± 0.15	8.74 ± 0.15				11.
9560	4.05		2.0 ± 0.2	-0.54	8.47	> 8.40					12.
9600											13.
9450	4.00		(2.0)	-0.56 ± 0.05							14.
9550 ± 50	3.95 ± 0.05		(2.0)	-0.50							15.
9600 ± 180	4.00 ± 0.10										16 ^a .
9600 ± 180	3.80 ± 0.30										16 ^b .
9830 ± 320											17 ^a .
9660											17 ^b .
9660 ± 140								3.24 ± 0.07			18 ^a .
9469								3.20			18 ^b .
9553 ± 111								3.28 ± 0.01			19.
(9430)	3.95 ± 0.20		1.50 ± 0.30	-0.57	8.46 ± 0.13	8.00 ± 0.02	9.01 ± 0.14				20.
(9650)	(3.95)	2.54 ± 1.21	(2.0)	(-0.50)	(8.42)	(8.00)	(8.74)	3.35 ± 0.20	61 ± 9	2.79 ± 0.17	21.

1. Blackwell et al. (1980); 2. Dreiling & Bell (1980); 3. Sadakane & Nishimura (1981); 4. Lambert et al. (1982); 5. Moon (1985); 6. Moon & Dworetzky (1985); 7. Gigas (1986); 8. Volk & Cohen (1989); 9. Adelman & Gulliver (1990); 10. Lemke (1990); 11. Venn & Lambert (1990); 12. Hill & Landstreet (1993); 13. Napiwotzki et al. (1993); 14. Smith & Dworetzky (1993); 15. Castelli & Kurucz (1994); 16. Smalley & Dworetzky (1995); 17. Sokolov (1995); 18. di Benedetto (1998); 19. Ciardi et al. (2001); 20. Qiu et al. (2001); 21. present results

their abundances for carbon, nitrogen, oxygen and iron were respectively: $\varepsilon(\text{C}) = 8.42 \pm 0.15$, $\varepsilon(\text{N}) = 8.00 \pm 0.15$, $\varepsilon(\text{O}) = 8.74 \pm 0.15$ and $[\text{Fe}/\text{H}] = -0.53 \pm 0.15$.

– Deduced parameters:

Our angular diameter derived from the ISO-SWS spectrum corresponds to the IRFM value from Blackwell et al. (1980). The same note as made in Sect. 3.4.4 concerning the luminosity and radius values mentioned by Volk & Cohen (1989) can be made: since the parallax value mentioned by Hoffleit & Jaschek (1982) ($\pi = 133 \text{ mas}$) only differs with the Hipparcos' value by a factor 1.03, the values for R and L are in close agreement. This can also be said for the radius value given by Dreiling & Bell (1980), who too have used the parallax of Hoffleit & Jaschek (1982). The new relation established by Moon (1985) results in stellar radius values which are somewhat lower than our deduced value and the values mentioned by Moon (1985) and Volk & Cohen (1989).

4. Conclusion

The five warmest stars in a sample of 16 stars — used for the calibration of the detectors of ISO-SWS — have been discussed spectroscopically. The absence of molecular features and the presence of atomic features whose oscillator strengths are not well-known rendered the determination of the effective temperature, gravity, microturbulent velocity, metallicity and the abundance of C, N, and O from the ISO-SWS data unfeasible. Good-quality published values were then used for the computation of the synthetic

spectra. In general, no more discrepancies than the ones reported in Decin et al. (2002) have been detected. A comparison with other — lower resolution — ISO-SWS data revealed a rather good relative agreement ($\sim 2\%$), but the absolute flux-level and so the deduced angular diameter could differ by up to 16%. Nevertheless, the angular diameter, luminosity and stellar radius deduced from the ISO-SWS data are in good agreement with other published values deduced from other data and/or methods.

Since this research has shown clearly that the available oscillator strengths of atomic transitions in the infrared are at the moment still very inaccurate, one of us (J. S.) has worked on a new atomic linelist by deducing new oscillator strengths from the high-resolution ATMOS spectrum of the Sun ($625 - 4800 \text{ cm}^{-1}$) (Sauval 2002). This new atomic linelist will be presented in Paper V of this series.

Acknowledgements. LD acknowledges support from the Science Foundation of Flanders. This research has made use of the SIMBAD database, operated at CDS, Strasbourg, France and of the VALD database, operated at Vienna, Austria. It is a pleasure to thank the referees, J. Hron and F. Kupka, for their careful reading of the manuscript and for their valuable suggestions.

References

- Abia, C., Rebolo, R., Beckman, J. E., & Crivellari, L. 1988, *A&A*, 206, 100
 Achmad, L., de Jager, C., & Nieuwenhuijzen, H. 1991, *A&A*, 249, 192

- Adelman, S. J. & Gulliver, A. F. 1990, *ApJ*, 348, 712
- Becker, S. A. 1981, *ApJS*, 45, 475
- Bell, R. A. & Dreiling, L. A. 1981, *ApJ*, 248, 1031
- Bessell, M. S., Castelli, F., & Plez, B. 1998, *A&A*, 333, 231
- Blackwell, D. E., Petford, A. D., & Shallis, M. J. 1980, *A&A*, 82, 249
- Blackwell, D. E. & Shallis, M. J. 1977, *MNRAS*, 180, 177
- Boyarchuk, A. A. & Lyubimkov, L. S. 1983, *Astrophysics*, 18, 228
- Brown, J. A., Tomkin, J., & Lambert, D. L. 1983, *ApJ*, 265, L93
- Brown, R. H., Davis, J., & Allen, L. R. 1974, *MNRAS*, 167, 121
- Castelli, F. & Kurucz, R. L. 1994, *A&A*, 281, 817
- Chmielewski, Y., Friel, E., Cayrel de Strobel, G., & Bentolila, C. 1992, *A&A*, 263, 219
- Ciardi, D. R., van Belle, G. T., Akeson, R. L., et al. 2001, *ApJ*, 559, 1147
- Claret, A. & Gimenez, A. 1995, *A&AS*, 114, 549
- Code, A. D., Bless, R. C., Davis, J., & Brown, R. H. 1976, *ApJ*, 203, 417
- Cohen, M., Walker, R. G., Barlow, M. J., & Deacon, J. R. 1992a, *AJ*, 104, 1650
- Cohen, M., Walker, R. G., & Witteborn, F. C. 1992b, *AJ*, 104, 2030
- Cohen, M., Witteborn, F. C., Bregman, J. D., et al. 1996a, *AJ*, 112, 241
- Cohen, M., Witteborn, F. C., Carbon, D. F., et al. 1996b, *AJ*, 112, 2274
- Cohen, M., Witteborn, F. C., Walker, R. G., Bregman, J. D., & Wooden, D. H. 1995, *AJ*, 110, 275
- Decin, L. 2000, PhD thesis, University of Leuven
- Decin, L., Vandebussche, B., Waelkens, C., et al. 2002, *A&A*, in press, (Paper II)
- Decin, L., Waelkens, C., Eriksson, K., et al. 2000, *A&A*, 364, 137
- Demarque, P., Guenther, D. B., & van Altena, W. F. 1986, *ApJ*, 300, 773
- Desikachary, K. & Hearnshaw, J. B. 1982, *MNRAS*, 201, 707
- di Benedetto, G. P. 1998, *A&A*, 339, 858
- di Benedetto, G. P. & Rabbia, Y. 1987, *A&A*, 188, 114
- Dreiling, L. A. & Bell, R. A. 1980, *ApJ*, 241, 736
- Edvardsson, B. 1988, *A&A*, 190, 148
- El Eid, M. F. 1994, *A&A*, 285, 915
- Engelke, C. W. 1992, *AJ*, 104, 1248
- England, M. N. 1980, *MNRAS*, 191, 23
- Feuchtgruber, H. 1998, Status of AOT01 AOT band order ratios and related data (ISO-SWS online documentation)
- Flannery, B. P. & Ayres, T. R. 1978, *ApJ*, 221, 175
- Furenlid, I. & Meylan, T. 1990, *ApJ*, 350, 827
- Gadun, A. S. 1994, *Astronomische Nachrichten*, 315, 413
- Gardiner, R. B., Kupka, F., & Smalley, B. 1999, *A&A*, 347, 876
- Geller, M. 1992, A High-Resolution Atlas of the Infrared Spectrum of the Sun and Earth Atmosphere from Space. Volume III. Key to Identification of Solar Features (Washington, D.C. : NASA, Scientific and Technical Information Division)
- Gigas, D. 1986, *A&A*, 165, 170
- Girardi, L., Bressan, A., Bertelli, G., & Chiosi, C. 2000, *A&AS*, 141, 371
- Gunson, M. R., Abbas, M. M., Abrams, M. C., et al. 1996, *Geoph. Res. Lett.*, 23, 2333
- Gustafsson, B., Bell, R. A., Eriksson, K., & Nordlund, Å. 1975, *A&A*, 42, 407
- Hill, G. M. & Landstreet, J. D. 1993, *A&A*, 276, 142
- Hill, V., Andrievsky, S., & Spite, M. 1995, *A&A*, 293, 347
- Hirata, R. & Horaguchi, T. 1995, Atomic spectral line list (internet: <http://cdsweb.u-strasbg.fr/htbin/Cat?VI/69>)
- Hoffleit, D. & Jaschek, C. 1982, The Bright Star Catalogue (The Bright Star Catalogue, New Haven: Yale University Observatory (4th edition), 1982)
- Holweger, H. & Rentzsch-Holm, I. 1995, *A&A*, 303, 819
- Hui-Bon-Hoa, A., Burkhart, C., & Alecian, G. 1997, *A&A*, 323, 901
- Johnson, H. L., Iriarte, B., Mitchell, R. I., & Wisniewskij, W. Z. 1966, *Communications of the Lunar and Planetary Laboratory*, 4, 99
- Kamper, K. W. & Wesselink, A. J. 1978, *AJ*, 83, 1653
- Lambert, D. L., Roby, S. W., & Bell, R. A. 1982, *ApJ*, 254, 663
- Leech, K., Kester, D., Shipman, R., et al. 2002, in The ISO Handbook. Volume V. SWS - The Short Wavelength Spectrometer, ed. K. Leech
- Lemke, M. 1990, *A&A*, 240, 331
- Lester, J. B., Gray, R. O., & Kurucz, R. L. 1986, *ApJS*, 61, 509
- Linsky, J. L. & Ayres, T. R. 1978, *ApJ*, 220, 619
- Luck, R. E. 1979, *ApJ*, 232, 797
- Luck, R. E. & Lambert, D. L. 1985, *ApJ*, 298, 782
- Lyubimkov, L. S. & Boyarchuk, A. A. 1984, *Astrophysics*, 19, 385
- Malagnini, M. L. & Morossi, C. 1990, *A&AS*, 85, 1015
- . 1997, *A&A*, 326, 736
- McWilliam, A. 1990, *ApJS*, 74, 1075
- Moon, T. 1985, *Ap&SS*, 117, 261
- Moon, T. T. & Dworetzky, M. M. 1985, *MNRAS*, 217, 305
- Napiwotzki, R., Schönberner, D., & Wenske, V. 1993, *A&A*, 268, 653
- Neuforge-Verheecke, C. & Magain, P. 1997, *A&A*, 328, 261
- Plez, B., Brett, J. M., & Nordlund, Å. 1992, *A&A*, 256, 551
- Plez, B., Smith, V. V., & Lambert, D. L. 1993, *ApJ*, 418, 812
- Popper, D. M. 1980, *ARA&A*, 18, 115
- . 1993, *ApJ*, 404, L67
- Pottasch, E. M., Butcher, H. R., & van Hoesel, F. H. J. 1992, *A&A*, 264, 138
- Pourbaix, D., Neuforge-Verheecke, C., & Noels, A. 1999, *A&A*, 344, 172
- Qiu, H., Zhao, G., Chen, Y. Q., & Li, Z. W. 2001, *A&A*, 548, 953

- Rentzsch-Holm, I. 1997, *A&A*, 317, 178
- Russell, S. C. & Bessell, M. S. 1989, *ApJS*, 70, 865
- Sadakane, K. & Nishimura, M. 1981, *PASJ*, 33, 189
- Sadakane, K. & Ueta, M. 1989, *PASJ*, 41, 279
- Sauval, A. J. 2002, Data file of IR solar atomic lines (unpublished results)
- Smalley, B. & Dworetsky, M. M. 1993, *A&A*, 271, 515
- . 1995, *A&A*, 293, 446
- Smith, K. C. & Dworetsky, M. M. 1993, *A&A*, 274, 335
- Smith, V. V. & Lambert, D. L. 1985, *ApJ*, 294, 326
- . 1986, *ApJ*, 311, 843
- Soderblom, D. R. 1986, *A&A*, 158, 273
- Sokolov, N. A. 1995, *A&AS*, 110, 553
- Spite, F., Spite, M., & Francois, P. 1989, *A&A*, 210, 25
- Trimble, V. & Bell, R. A. 1981, *QJRAS*, 22, 361
- Venn, K. A. & Lambert, D. L. 1990, *ApJ*, 363, 234
- Volk, K. & Cohen, M. 1989, *AJ*, 98, 1918
- Witteborn, F. C., Cohen, M., Bregman, J. D., et al. 1999, *AJ*, 117, 2552